

Database for inelastic collisions of sodium atoms with electrons, protons, and multiply charged ions

K. Igenbergs^a, J. Schweinzer^b, I. Bray^c, D. Bridi^a, F. Aumayr^{a,*}

^a Institut für Allgemeine Physik, Technische Universität Wien, Wiedener Hauptstrasse 8-10, A-1040 Vienna, Austria

^b Max-Planck-Institut für Plasmaphysik, Boltzmannstrasse 2, D-85748 Garching, Germany

^c Curtin University of Technology, GPO Box U1987, Perth, WA 6845, Australia

ARTICLE INFO

Article history:

Available online 18 September 2008

ABSTRACT

The available experimental and theoretical cross section data for inelastic collision processes of ground (3s) and excited (3p, 4s, 3d, 4p, 5s, 4d, and 4f) state Na atoms with electrons, protons, and multiply charged ions have been collected and critically assessed. In addition to existing data, electron-impact cross sections, for both excitation and ionization, have been calculated using the convergent close-coupling approach. In the case of proton-impact cross section, the database was enlarged by new atomic-orbital close-coupling calculations. Both electron-impact and proton-impact processes include excitation from the ground state and between excited states ($n = 3-5$). For electron-impact, ionization from all states is also considered. In the case of proton-impact electron loss, cross sections (the sum of ionization and single-electron charge transfer) are given. Well-established analytical formulae used to fit cross sections, published by Wutte et al. and Schweinzer et al. for collisions with lithium atoms, were adapted to sodium. The “recommended cross sections” for the processes considered have been critically evaluated and fitted using the adapted analytical formulae. For each inelastic process the fit parameters determined are tabulated. We also present the assessed data in graphical form. The criteria for comprehensively evaluating the accuracy of the experimental data, theoretical calculations, and procedures used in determining the recommended cross sections are discussed.

© 2008 Elsevier Inc. All rights reserved.

* Corresponding author. Fax: +43 1 58801 13499.
E-mail address: aumayr@iap.tuwien.ac.at (F. Aumayr).

Contents

1. Introduction	982
2. Basic description of the theoretical methods applied	982
2.1. Convergent close-coupling method for electron-impact collisions	982
2.2. Atomic-orbital close-coupling method for ion-impact collisions	983
3. Presentation of the data	983
3.1. General remarks on credibility and weighted fitting	983
3.2. Collisions with electrons	983
3.3. Collisions with protons	986
3.4. Scaling relations for collisions with multiply charged ions	987
Acknowledgments	990
References	990
Explanation of Tables	991
Explanation of Graphs	992

Tables

1. Fit parameters for electron-impact target-excitation cross sections of Na($nl \rightarrow n'l'$); $n, n' = 3-5$	993
2. Fit parameters for electron-impact target-ionization cross sections of Na(nl); $n = 3-5$	994
3. Fit parameters for proton-impact target-excitation cross sections of Na($nl \rightarrow n'l'$); $n, n' = 3-5$	995
4. Fit parameters for proton-impact target-electron-loss cross sections of Na(nl); $n = 3-5$	996

Graphs

1-28. Electron-impact target-excitation cross sections of Na($nl \rightarrow n'l'$); $n, n' = 3-5$	997
29-36. Electron-impact target-ionization cross sections from Na(nl); $n = 3-5$	1004
37-64. Proton-impact target-excitation cross sections from Na($nl \rightarrow n'l'$); $n, n' = 3-5$	1006
65-72. Proton-impact target-electron-loss cross sections from Na(nl); $n = 3-5$	1013

1. Introduction

The work on this database is motivated not only by the fundamental interest in the matter, but also by the need for reliable cross sections for the evaluation of plasma edge diagnostics in magnetically confined fusion plasmas by means of active neutral sodium beam spectroscopy. The basic experimental, theoretical, and computational concepts are based on and refer to the earlier work on neutral lithium-beam diagnostics [1–8]. Similar to lithium, injection of a fast neutral sodium beam into the edge of a magnetically confined plasma is able to deliver diagnostic information such as radial electron density profiles and spatially and time-resolved impurity ion concentrations [9–11]. A series of recent experiments at the ASDEX Upgrade tokamak and their preliminary analysis have shown that sodium beams are even better suited for this purpose than lithium. The interpretation of the emission line Na(3p–3s) of injected atoms, which provides information on the plasma edge density, requires a good knowledge of all inelastic collision processes involved. Therefore, the success of this plasma edge diagnostic method strongly depends on the availability of reliable cross sections of inelastic collisions of sodium atoms with plasma particles, namely, electron, protons, and multiply charged impurity ions.

The scope of the cross section database presented for collision processes of sodium atoms is mainly determined by the requirements of the Na-beam diagnostics. For the modeling of the diagnostic Na beam, eight bound Na states, 3s, 3p, 4s, 3d, 4p, 5s, 4d, and 4f are sufficient. The inelastic collision processes involving these eight Na states, are electron-impact target excitation, electron-impact target ionization, proton-impact target excitation, and proton-impact target electron loss. In the following sections, data for these processes will be presented. Sorting according to quantum numbers nl will be applied.

For many processes no cross sections could be found in the literature. Therefore we used advanced theoretical methods in this work to derive accurate cross sections for all inelastic processes

involving collisions with Na atoms (see Section 2). These theoretical results are critically assessed by comparing them with the most reliable experimental data available. In all cases good or at least satisfactory agreement between experiment and theory is found. Thus it is plausible to have a comparable level of confidence in the theoretical cross sections where experimental validation is not feasible.

The recommended cross sections for the processes considered are a product of either a critical assessment of available experimental and theoretical data or these new calculations alone. They are presented by giving their analytical fit expressions and tabulating the values of all parameters entering these analytic fits. We also present the recommended cross sections in graphical form together with the cross section data used for their generation.

2. Basic description of the theoretical methods applied**2.1. Convergent close-coupling method for electron-impact collisions**

In the past 20 years there has been an enormous progress both in the theoretical description of electron-atom scattering and the computational adaptation of these theories. The latter is, of course, strongly supported by the more and more powerful computational resources which allow large close-coupling basis sets. Here we use the convergent close-coupling method (CCC) developed by Bray and Stelbovics [12]. Briefly this method uses a set of square-integrable basis states, obtained by diagonalizing the target Hamiltonian in an orthogonal L^2 Laguerre basis, to expand the total wave function of the system. For the sodium target we assume that the frozen-core Hartree-Fock Hamiltonian is a sufficiently accurate representation. Hence, we treat sodium as essentially a one-electron target and electron-sodium scattering as a three-body problem.

The CCC method has already been extensively tested for inelastic electron-sodium scattering [13]. It reproduces closely the very

detailed measurements of 3p excitation and the total ionization cross section. Thus, we have very good reasons to believe in the accuracy of the CCC method in evaluating integrated cross sections for all discrete transitions at all energies. The key issue is obtaining convergence for the transitions of interest with increasing number of expansion states [14]. Generally, the smaller the cross section, the larger the calculation necessary to obtain an accurate result. In practice, we choose a sufficiently large set of states to obtain accurately the most important transitions of interest.

2.2. Atomic-orbital close-coupling method for ion-impact collisions

For ion-impact cross-section calculations, we adopted the semi-classical impact-parameter formalism of the close-coupling (CC) method, assuming straight line trajectories for the projectiles [15–17]. The time-dependent electronic wave function is expanded in projectile- and target-centered traveling orbitals which need not necessarily be eigenstates of the corresponding atomic Hamiltonian. Thus, in addition to the atomic-orbital (AO) method, so-called pseudostates (PS) are also included in our two-center expansion model. While AO represent the bound spectrum of the separated atoms of relevance for the considered inelastic collision process, PS are chosen to account for the formation of transient molecular orbitals as well as to represent ionization channels. The CC calculation always starts from a linear combination of states which results from diagonalization of the atomic Hamiltonians within the given set of basis states on each center.

The interaction between the core electrons and the “active” electron is described by a model potential. The experimental energy level diagram of Na ($n \leq 5$) is accurately reproduced by the eigenvalues of the model potential. One-center couplings between projectile states induced by the electric field of the Na^+ core are calculated in good approximation by assuming a pure Coulomb interaction potential.

For collisions of H^+ with $\text{Na}(nl)$, cross sections for single-electron capture (SEC), target excitation (EXC), and ionization (ION) are mainly derived from AO calculations involving 44 states centered on the proton core and 83 states (AO44_83) centered on the Na^+ core. This main basis set is used for calculations with initial Na target states 3s, 3p, 3d, 4s, and 4p for impact energies between 1 and 500 keV. On both centers, atomic states with principal quantum numbers $n \leq 5$ are represented in the calculations. All other states are PS, which are orthogonal to the included atomic states of the basis and thus will overlap with higher excited bound states as well as with continuum states. The projection of such discrete non-bound pseudo-states on the continuum is the basis for the calculation of ionization cross sections. Another basis set AO70_29 is used to check the convergence of results as well as to extend the impact energy range towards 0.2 keV. In addition to the two-center calculations, pure one-center calculations without projectile centered states (AO0_83) were also performed. These calculations were used to derive EXC and ION cross sections at impact energies of 200–1000 keV with considerable less computational effort. In this high-impact-energy region, the EXC and ION process is completely decoupled from electron capture, and thus results from AO0_83 do not differ from those of the much more elaborate calculation AO44_83.

Cross sections for target electron loss (ELOSS, that is SEC + ION) are obtained by summing over all cross sections for population of projectile-centered states and the direct ionization cross section of the Na atom. Results for ELOSS from the AO44_83 calculations are believed to be convergent for impact energies of 1–15 keV. For higher impact energies the ELOSS cross section is dominated by the ionization process, which is not sufficiently well described in the basis set applied here. Therefore, at high-impact energies, ELOSS cross sections are underestimated by our AO calculations.

This was taken into account in the process of establishing recommended cross sections (see Section 3.3).

In general, the coupled equations are solved along straight line trajectories $R = vt + b$ (R being the internuclear distance and v the velocity) from $vt = -300a_0$ to $300a_0$ (a_0 being the Bohr radius) and for impact parameters b from $0.3a_0$ to $50a_0$. However, for dipole-allowed EXC cross sections with small ΔE values, much larger meshes had to be used. In particular, the AO0_83 calculations were done between $vt = -800a_0$ and $800a_0$ with impact parameters up to $200a_0$.

Similar calculations were performed for He^{2+} and Be^{4+} colliding with $\text{Na}(3s, 3p)$. Results from these calculations were used to check the behavior of EXC and ELOSS cross section with respect to the projectile charge q (see Section 3.4).

3. Presentation of the data

3.1. General remarks on credibility and weighted fitting

The most important excitation and ionization cross sections induced by the collisions of both electron and proton impact on sodium have been subject to a large number of experimental and theoretical studies. Obviously, the various methods imply different margins of error. For a comprehensive evaluation of the cross sections, it became necessary to judge the credibility and to weight the cross sections accordingly in the fit leading to the recommended cross section. The following general guidelines were applied to this process. First, it is a known fact that first-order Plane Wave Born Approximation (PWBA) cross sections excellently predict the asymptotic cross sections in the high-energy tail and but show a large discrepancy in the low-energy region. Thus, PWBA cross sections were strongly weighted above a certain energy limit and very poorly below this limit. Second, the better the data were compatible with the general trend of all collected cross sections of one transition, the stronger they were weighted in the fit. Third, data predating 1980 were generally considered to be not as accurate as more recent ones.

3.2. Collisions with electrons

The database presented consists of comprehensively evaluated data found in the scientific literature. The quality and reliability of the database is further enhanced by including the CCC calculations into the critical data assessment process. All calculations are performed in the impact-energy range from the excitation threshold up to 10 keV.

Experimental data exist for electron-impact excitation processes from the ground state to 3p, 3d, 4s, 4p, 4d, and 5s. Additionally, experimental data for $e^- + \text{Na}(3p) \rightarrow e^- + \text{Na}(3d)$ are available.

Representation of the cross sections is achieved by applying the Levenberg-Marquardt method for non-linear fits [18] implemented in gnuplot [19] and using the following analytic expression with seven parameters (A_1, \dots, A_7)

$$\sigma_{e^-}^{\text{EXC}}(e/\text{eV})[\text{cm}^2] = \frac{A_7 \cdot 10^{-16}}{E} \left[\frac{E - \Delta E}{E} \right]^{A_6} \cdot \left[\sum_{j=1}^4 \frac{A_j}{(E/\Delta E)^{j-1}} + A_5 \cdot \ln \left(\frac{E}{\Delta E} \right) \right] \quad \forall E > \Delta E \quad (1)$$

where ΔE is the excitation threshold energy. The fitting functions were chosen to assure asymptotically correct behavior both at low- and high-impact energies. The behavior in the low-energy region is mainly implemented by the second factor. It is thus essentially necessary that parameter A_6 does not take negative values. As a typical example for the quality of the fitting procedure, the result of the CCC calculation for a single EXC process ($\text{Na}(3s \rightarrow 3d)$) is

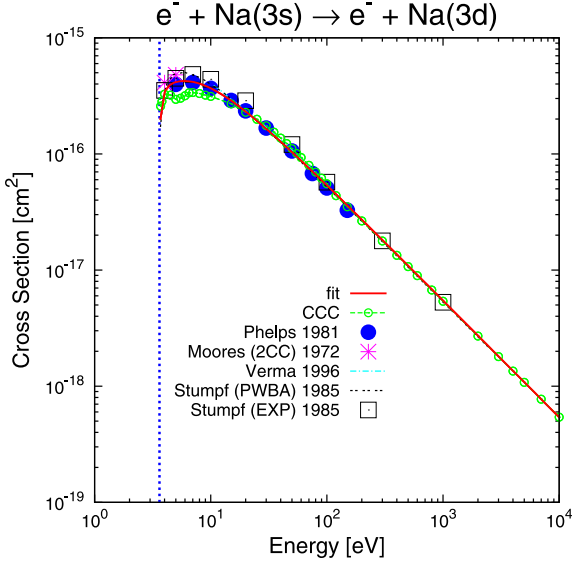


Fig. 1. Results from the CCC calculations for the $\text{Na}(3s \rightarrow 3d)$ electron-impact excitation in comparison with experimental and other theoretical data and the analytic fit (see Eq. (1) and Table 1).

presented in Fig. 1 together with the fit parameters according to Table 1. Deviations of the fit from the defining data points are, in general, below a few percent. In some cases there are data available for energies just above, but very close to the excitation threshold energy. The fits, though, all converge toward zero at threshold.

The collections of cross sections including the present CCC calculations are visualized in graphs (Graphs 1–28). In these graphs the excitation threshold energy of the corresponding transition is displayed by a vertical blue¹ single-dashed line. The accuracy of the experimental and theoretical data is limited according to the terms in Section 3.1. For the origin of the used references consult Table A.

The collection of electron-impact target ionization cross sections includes additional data only for ground state and first excited state ionization. Again, the deviations of the fit and the data points are essentially below a few percent, except very close to the threshold. This gave rise to the introduction of the low energy limit E_{low} , below which the fit cannot predict the trend of the cross section anymore. Thus, the final form of the used analytical fit formula for electron-impact target ionization with seven fit parameters (A_1, \dots, A_7), see Table 2, is

$$\sigma_{0,e}^{\text{ION}}(E/\text{eV})[\text{cm}^2] = \frac{A_7 \cdot 10^{-13}}{E \cdot I_{nl}} \cdot \left[A_5 \cdot \ln\left(\frac{E}{I_{nl}}\right) + A_6 \cdot \exp\left(-\frac{E}{I_{nl}}\right) + \sum_{j=1}^4 A_j \cdot \left(1 - \frac{I_{nl}}{E}\right)^{j-1} \right] \quad \forall E \geq E_{\text{low}}. \quad (2)$$

Neither this fit formula nor the CCC calculations take into account that at impact, energies above the binding energy of the 2s and 2p subshells inner-shell ionization occurs. We proceeded in the following way: first the available cross section data were collected and fitted and then the contribution of inner-shell ionization was added to the fitting curve. We used the Lotz formula (Eq. (3)) that provides an analytical evaluation of inner-shell ionization [20]. In this case the Lotz formula is outlined explicitly as follows:

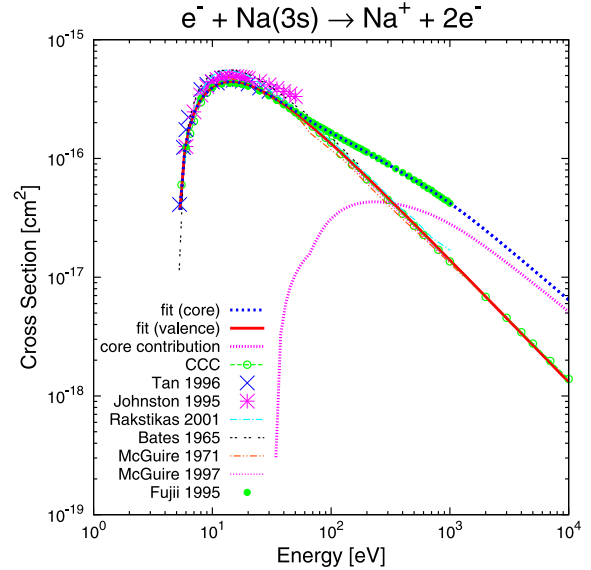


Fig. 2. Electron-impact target ionization from $\text{Na}(3s)$. The fit of the valence is plotted according to Eq. (2) and Table 2. The fit containing inner shell ionization ("fit with core") is plotted according to Eq. (4), where the core correction is added to Eq. (2) according to Eq. (3)) and Table D. The core fraction represents the contribution of inner-shell ionization according to Eq. (5). and Table D.

$$\begin{aligned} \sigma_{2p}^{\text{ION}}(E/\text{eV})[\text{cm}^2] &= q_{2p} \cdot L_1 \cdot 10^{-14} \cdot \frac{\ln(E/I_{2p})}{E \cdot I_{2p}} \\ &\cdot \{1 - L_2 \cdot \exp(-L_3(E/I_{2p} - 1))\} \\ \sigma_{2s}^{\text{ION}}(E/\text{eV})[\text{cm}^2] &= q_{2s} \cdot L_4 \cdot 10^{-14} \cdot \frac{\ln(E/I_{2s})}{E \cdot I_{2s}} \\ &\cdot \{1 - L_5 \cdot \exp(-L_6(E/I_{2s} - 1))\}. \end{aligned} \quad (3)$$

The input parameters to Eq. (3) according to [21] are $I_{2p} = 34$ eV and $I_{2s} = 67$ eV, the binding energies of 2p, respectively, 2s electrons, $q_{2p} = 6$ and $q_{2s} = 2$, the number of equivalent 2p, respectively, 2s electrons, and L_1, \dots, L_6 are sets of individual constants for the 2p, respectively, 2s subshell.

The overall formula for electron-impact target ionization is

$$\sigma_{e^-}^{\text{ION}}(E/\text{eV})[\text{cm}^2] = \begin{cases} \sigma_0^{\text{ION}} & \forall E_{\text{low}} \leq E \leq I_{2p} \\ \sigma_0^{\text{ION}} + \sigma_{2p}^{\text{ION}} & \forall I_{2p} \leq E \leq I_{2s} \\ \sigma_0^{\text{ION}} + \sigma_{2p}^{\text{ION}} + \sigma_{2s}^{\text{ION}} & \forall E \geq I_{2s}. \end{cases} \quad (4)$$

The constants in Eq. (3) have to be determined either by experiment, theory, or reasonable guesswork [21]. We were able to gather experimental data on ionization from the ground state in the energy region where inner-shell ionization occurs, see Ref. [22]. All other references are listed in Table B. We now used Eq. (2) to fit ionization of the valence electron without considering inner-shell ionization. This led to the red line² curve in Fig. 2. The parameters A_1, \dots, A_7 remained constant and we used

$$\sigma_{\text{core}}^{\text{ION}}(E/\text{eV})[\text{cm}^2] = \begin{cases} \sigma_{2p}^{\text{ION}} & \forall I_{2p} \leq E \leq I_{2s} \\ \sigma_{2p}^{\text{ION}} + \sigma_{2s}^{\text{ION}} & \forall E \geq I_{2s} \end{cases} \quad (5)$$

with variable parameters L_1, \dots, L_6 to fit the inner-shell contribution. The parameters obtained (see Table D) vary slightly from the original parameters presented by Lotz [20], but represent the experimental values excellently. We therefore used these new fit parameters (see Table D) to derive the core corrections in all ionization cross sections. In this way not only ionization including the

¹ For interpretation of the references to color in these graphs, the reader is referred to the web version of this paper.

² For interpretation of the references to color in this figure, the reader is referred to the web version of this paper.

Table A

Publications used for electron-impact target-excitation cross sections

Electron-impact target excitation					
Transition	Name	Published in	Referenced in	Weight in fit	Comment
3s → 3p	Buckman (1979)	[26]	[27]	Low	Experiment
	Enemark (1972)	[28]	—	High	Experiment
	Gould (1970)	[29]	[30]	Low	Calculation
	Karule (1970)	[31]	[30]	Low	Experiment
	Kim (2001)	[32]	—	Moderate	Below 100 eV: very low calculation
	Mitroy (1987)	[27]	—	Low	Calculation
	Moores (2CC) (1972)	[30]	—	Low	Two-center close-coupling calculation
	Moores (4CC) (1972)	[30]	—	Low	Four-center close-coupling calculation
	Phelps (1981)	[33]	—	High	Experiment
	Srivastava (1980)	[34]	—	Moderate	Experiment
	Zapesochnyi (1976)	[35]	[36]	Very low	Experiment
3s → 3d	Moores (2CC) 1972	[30]	—	Low	Two-center close-coupling calculation
	Phelps (1981)	[33]	—	High	Experiment
	Stumpf (PWBA) (1985)	[37]	—	Moderate	Born approximation calculation
	Stumpf (EXP) (1985)	[37]	—	High	Experiment
3s → 4s	Verma (1996)	[38]	—	Low	Calculation
	Moores (2CC) 1972	[30]	—	Low	Two center close-coupling calculation
	Phelps (1981)	[33]	—	High	Experiment
3s → 4p	Srivastava (1980)	[34]	—	Moderate	Experiment
	Phelps (1981)	[33]	—	High	Experiment
	3s → 4d	Phelps (1981)	[33]	High	Experiment
3p → 3d	Stumpf (1985)	[37]	—	Moderate	Experiment

The columns contain the following information: (1) transition in question, (2) name of the data in the graphs, (3) original reference, (4) if applicable, the publication where the used data were taken from, (5) weight in fit according to assigned credibility, and (6) comment.

Table B

References used for electron-impact target ionization cross sections

Electron-impact target ionization					
Ground state	Name	Published in	Referenced in	Weight in fit	Comment
3s	Bates (1965)	[39]	[40]	Low	Calculation
	Fujii and Srivastava (1995)	[22]	—	Very high	Experiment
	Johnston (1995)	[41]	—	Moderate	Experiment
	McGuire (1971)	[42]	—	Low	Calculation
	McGuire (1997)	[43]	—	Moderate	Calculation
	Rakstikas (2001)	[44]	—	High	Calculation
	Tan (1996)	[45]	—	High	Experiment
	Zapesochnyi (1968)	[46]	[45]	Low	Experiment
	Tan (1996)	[45]	—	High	Experiment
3p					

For description of column contents, see Table A.

Table C

References used for proton-impact target excitation

Proton-impact target excitation					
Transition	Name	Published in	Referenced in	Weight in fit	Comment
3s → 3p	Allen (1988)	[47]	[48]	Very high	Experiment
	Aumayr (1987)	[49]	—	Very high	Experiment
	Fritsch (1987)	[50]	[51]	High	Calculation
	Howald (1983)	[52]	—	Low	Experiment
	Jain (1995)	[53]	—	High	Calculation
	Jitschin (1986)	[54]	—	Low	Experiment
	Lavrov (1983)	[55]	[56]	Low	Experiment
	Shingal (AO) (1986)	[57]	—	High	Atomic-orbital calculation
	Shingal and Bransden (1987)	[51]	—	Low	Calculation
	Starý (1990)	[58]	—	Moderate	Calculation
	Theodosiou (1987)	[56]	—	Very low	Calculation
3s → 3d	Anderson (1979)	[59]	—	Moderate	Experiment
	Anderson (1985)	[60]	—	Moderate	Experiment
	Jain (1995)	[53]	—	High	Calculation
	Shingal and Bransden (1987)	[51]	—	High	Calculation
3s → 4s	Theodosiou (1987)	[56]	—	Low	Calculation
	Theodosiou (1987)	[56]	—	Low	Calculation
	Theodosiou (1987)	[56]	—	Low	Calculation
	Theodosiou (1987)	[56]	—	Low	Calculation
3s → 4p	Theodosiou (1987)	[56]	—	Low	Calculation
3s → 4d	Theodosiou (1987)	[56]	—	Low	Calculation
3s → 4f	Theodosiou (1987)	[56]	—	Low	Calculation

For description of column contents, see Table A.

Table D
Parameters for the Lotz formula, Eq. (3)

2p Electrons			2s Electrons		
L_1	L_2	L_3	L_4	L_5	L_6
3.49	0.81	0.087	10.8	0.46	1.5

The values vary slightly from the ones presented by Lotz [20], but represent the experimental values excellently.

core-correction but also pure valence ionization is represented for all transitions.

Fig. 2 presents ground-state electron-impact ionization. It shows very clearly that the contributions from the core electrons are substantial in the high-energy region and cannot be neglected. All ionization processes are shown in Graphs 29–36.

3.3. Collisions with protons

If the velocities of relative motion are the same, and are sufficiently high, the cross sections for proton–atom collisions are equal to the cross sections for the corresponding electron–atom collision. The electron-impact cross sections need to be scaled according to the formula [23]

$$E_{H^+} [\text{keV}] = 0.9165 \cdot E [\text{eV}] \cdot \left(1 - 0.5 \cdot \frac{\Delta E}{E} + \sqrt{1 - \frac{\Delta E}{E}} \right). \quad (6)$$

This scaling is appropriate in the asymptotic region at high energies where Born approximation cross sections for H^+ and e^- are the same at the same relative velocity of collision partners, since in this region the mechanism of direct excitation is the same for electrons and protons (see Fig. 3). In the graphs depicting proton-impact target excitation cross sections, these scaled electron-impact cross sections are labeled “scaled CCC.”

When the impact energy of the incident proton is lowered, a change from direct excitation to the forming of a quasi-molecule takes place. In this energy region the scaling relation (6)

is no longer valid and single-electron charge transfer becomes the dominant process. Originating from this interference of SEC and EXC channels, the cross sections show oscillations. Due to this more complex behavior, a formula with 12 fit parameters has to be used for proton-impact target excitation, specifically

$$\sigma_{H^+}^{\text{EXC}} (E/\text{keV}) [\text{cm}^2] = A_1 \cdot 10^{-16} \left\{ \frac{e^{-A_2/E} \cdot (A_{12} + \ln(A_{11} + A_3 E))}{E} \right. \\ \left. + A_4 \cdot \frac{e^{-A_5 E}}{E^{A_6}} + A_7 \cdot \frac{e^{-A_8/E}}{1 + A_9 \cdot E^{A_{10}}} \right\} \forall E \geq E_{\text{low}}. \quad (7)$$

The fit parameters for EXC processes $\text{Na}(nl \rightarrow n'l')$ in collisions with H^+ are listed in Table 3. The theoretical data defining the fit for the $\text{Na}(3p \rightarrow 3d)$ EXC cross section are presented in Fig. 3 together with the fitted curve and the scaled electron-impact cross section derived from CCC results by using the scaling relation from Ref. [23] (Eq. (6)). The AO data from $\text{Na}(nl \rightarrow n'l')$ EXC processes with $n = 3–5$ and $n' = 3–5$ are shown in graphs 37–64 together with the fits and compared with experimental and other theoretical data where available and the scaled CCC cross sections; the comparison will be further discussed in the next section. For references of used data see Table C.

Proton-impact target electron loss (ELOSS) is the sum of proton-impact ionization and proton-impact single-electron capture. There are no ELOSS data available in the literature. However there are data for both proton-impact SEC and ION. Figs. 4–6 show, using the ground state $\text{Na}(3s)$ as an example, how our new AO–CC calculations predict both SEC and ION cross sections excellently and how the SEC and ION fits, if added together, agree excellently with our AO–CC calculation of ELOSS. ION and SEC cross sections were fitted using the same formula

$$\sigma_{H^+}^{\text{ION,SEC}} (E/\text{keV}) [\text{cm}^2] = A_1 \cdot 10^{-16} \left\{ \frac{e^{-A_2/E} \cdot (A_{12} + \ln(A_{11} + A_3 E))}{E} \right. \\ \left. + A_4 \cdot \frac{e^{-A_5 E}}{E^{A_6}} + A_7 \cdot \frac{e^{-A_8/E}}{1 + A_9 \cdot E^{A_{10}}} \right\} \forall E \geq E_{\text{low}}. \quad (8)$$

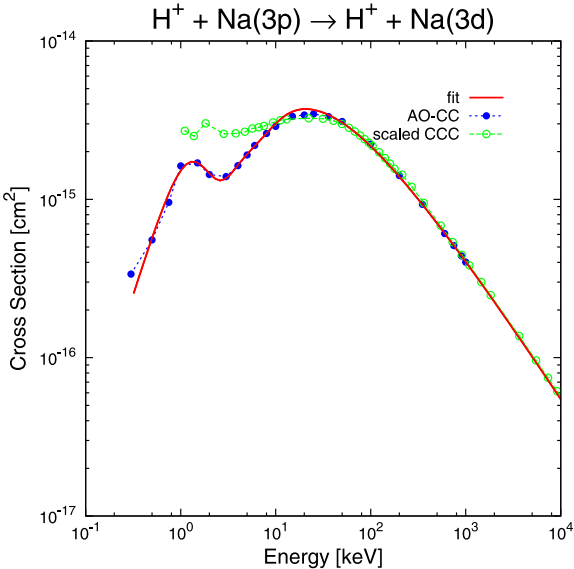


Fig. 3. Results from atomic-orbital close-coupling calculations for the $\text{Na}(3p \rightarrow 3d)$ excitation process in collisions of H^+ with $\text{Na}(3p)$ in comparison with the corresponding fit (Eq. (7), Table 3) and with the scaled electron impact cross section. The latter has been derived from the new CCC calculations by applying the scaling relation from [23] (Eq. (6)).

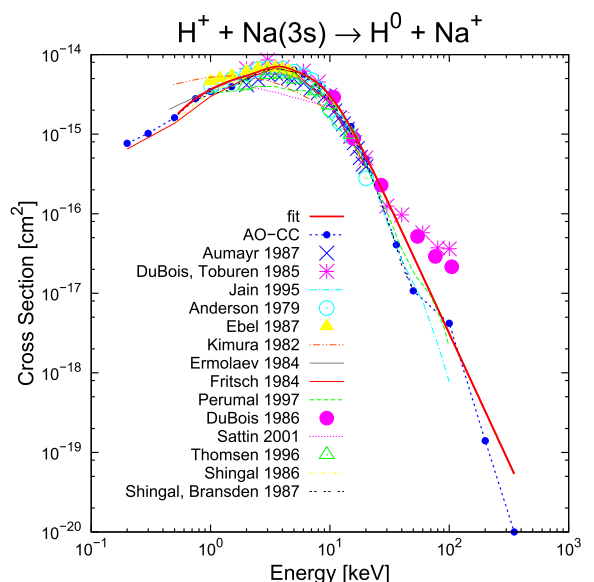


Fig. 4. Proton-impact single-electron capture cross sections from $\text{Na}(3s)$. For references see Table F.

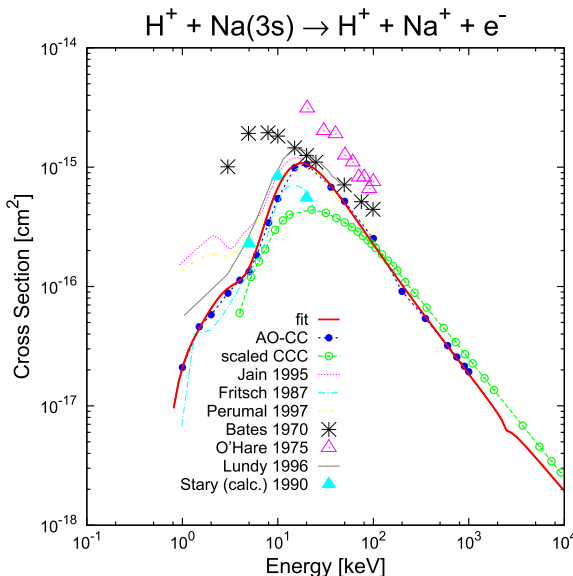


Fig. 5. Proton-impact target ionization cross sections from Na(3s). For references see Table G.

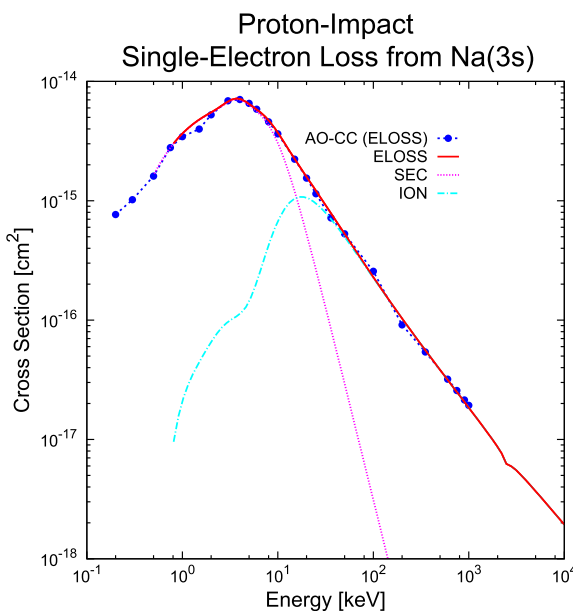


Fig. 6. Proton-impact target electron loss cross sections from Na(3s). AO-CC (ELOSS): present AO-CC calculations. ELOSS: fit for electron loss (Eq. (9)). SEC: fit for single-electron capture (Eq. (8)). ION: fit for ionization (Eq. (8)).

with the fit parameters A_1 – A_{12} , tabulated in Table E, and E_{low} again the energy limit in the low-energy region. For used references see Tables F and G.

Finally the combined cross section (i.e., target electron loss) was fitted using the following formula

$$\sigma_{\text{H}^+}^{\text{ELOSS}} (E/\text{keV}) [\text{cm}^2] = A_1 \cdot 10^{-16} \left\{ \frac{e^{-A_2/E} \cdot \ln(1 + A_3 E)}{E} + A_4 \cdot \frac{e^{-A_5 E}}{E^{A_6}} \right\} \quad \forall E \geq E_{\text{low}} \quad (9)$$

where A_1 – A_6 are the fit parameters, see Table 4, and E_{low} , the limit of the validity of the fit in the low-energy region. All ELOSS cross sections are shown in Graphs 65–72.

The data for ELOSS involve processes with initial Na(nl) $\forall n \leq 5$. They have been compared with scaled CCC calculations of electron-impact ionization cross sections. The agreement between these data is expected to be good in the energy region above ≈ 100 keV where ionization is the dominant process in ELOSS. Unfortunately, the agreement is not always as good as hoped. This is due to the insufficient representation of ionization channels in the AO-CC calculations. Furthermore the AO calculations include neither SEC from Na inner shells nor ionization of the latter.

3.4. Scaling relations for collisions with multiply charged ions

A realistic fusion plasma is always polluted by a certain amount of impurity ions. Thus, to achieve satisfactory quality in simulations, it is necessary to include sodium-impurity ion collisions. The behavior of EXC cross sections with respect to a rescaling relation with projectile charge state q and mass m (in amu), derived from a three-state close-coupling dipole approximation [24] [25]. This scaling formula, with respect to the electron binding energy E_b of the initial state of the target sodium and the charge of the fully stripped projectile, has been derived for single electron charge transfer from excited hydrogen atoms H(n) in a wide impact energy range. The same reduced impact energy and cross section are introduced for target excitation [17]

$$E_{\text{red.}}^{\text{EXC}} = \frac{E}{q}, \quad \sigma_{\text{red.}}^{\text{EXC}} = \frac{\sigma}{q} \quad (10)$$

and for single-electron capture [17]

$$E_{\text{red.}}^{\text{ELOSS}} = \frac{n^2 \cdot E}{\sqrt{q}}, \quad \sigma_{\text{red.}}^{\text{ELOSS}} = \frac{\sigma}{n^4 q} \quad (11)$$

where n is the principal quantum number of the sodium target with respect to the binding energy ($n = (2E_b)^{-1/2}$) [17]. These well-proven scaling relations have been applied to collisions involving He $^{2+}$ and Be $^{4+}$ projectiles. Fig. 7 shows calculated excitation cross sections (Na(3s) → Na(3p)) by ion impact, whereas Fig. 8 shows the corresponding reduced cross sections (in terms of Eq. (10)). In the energy region above reduced energies E/q of about 3 keV/amu, the fit of the proton-impact cross section (Eq. (7), Table 3) represents the other reduced cross sections well. A similar behavior can be observed for excitation from Na(3p) to Na(3d) and to Na(4s), see Figs. 9 and 10, respectively. The q -scaling typically breaks down below reduced

Table E

Fit parameters for proton-impact target ionization (ION) and single-electron capture (SEC) from Na(3s)

	E_{low}	A_1	A_2	A_3	A_4	A_5	A_6	A_7	A_8	A_9	A_{10}	A_{11}	A_{12}
ION	1	8.389	8.83	-7.95×10^{-4}	-0.179	0.4266	-2.554	1.13	2.095	1.52×10^{-3}	1.998	2.02	21.21
SEC	0.5	24.21	1.0	0	1.68×10^{-3}	5.02	-18.34	3.342	0.798	8.155×10^{-4}	3.25	1.0	0

Table F

References used for proton-impact single-electron capture cross sections

Proton-impact single-electron capture					
Ground state	Name	Published in	Referenced in	Weight in fit	Comment
3s	Anderson (1979)	[59]	[53]	High	Experiment
	Aumayr (1987)	[49]	—	Very high	Experiment
	DuBois and Toburen (1985)	[61]	—	Very high	Experiment
	DuBois (1986)	[62]	—	Moderate	Experiment
	Ebel (1987)	[63]	—	Moderate	Experiment
	Ermolaev (1984)	[64]	[63]	Moderate	Calculation
	Fritsch (1984)	[65]	—	Very high	Calculation
	Jain (1995)	[53]	—	Very high	Calculation
	Kimura (1982)	[66]	[63]	Low	Calculation
	Permal (1997)	[67]	—	Moderate	Calculation
	Sattin (2001)	[68]	—	Very low	Calculation
	Shingal (1986)	[57]	—	High	Calculation
	Shingal and Bransden (1987)	[51]	—	High	Calculation
	Thomsen (1996)	[69]	[68]	High	Experiment

For description of column contents, see Table A.

Table G

References used for proton-impact target ionization cross sections

Proton-impact target ionization					
Ground state	Name	Published in	Referenced in	Weight in fit	Comment
3s	Bates (1970)	[70]	[67]	Low	Experiment
	Fritsch (1987)	[50]	[53]	High	Calculation
	Jain (1995)	[53]	—	Moderate	Calculation
	Lundy (1996)	[71]	—	Moderate	Calculation
	O'Hare (1975)	[72]	—	Low	Experiment
	Permal (1997)	[67]	—	Moderate	Calculation
	Stary (calcd) (1990)	[58]	—	Low	Optical potential calculations

For description of column contents, see Table A.

energies $E/q < 3$ keV/amu. In this low impact energy range no general behavior of EXC cross sections with respect to q can be expected.

Figs. 11 and 12 show reduced ELOSS cross sections from Na(ns) and Na(np) initial states, respectively. In the reduced energy region

below 10 keV/amu, reduced ELOSS cross sections from Na(ns) become almost independent from the energy of the incident particle, except for the $H^+ - Na(3s)$ case (see Fig. 11). The behavior of the latter is typical for a nonresonant SEC, whereas all other collision sys-

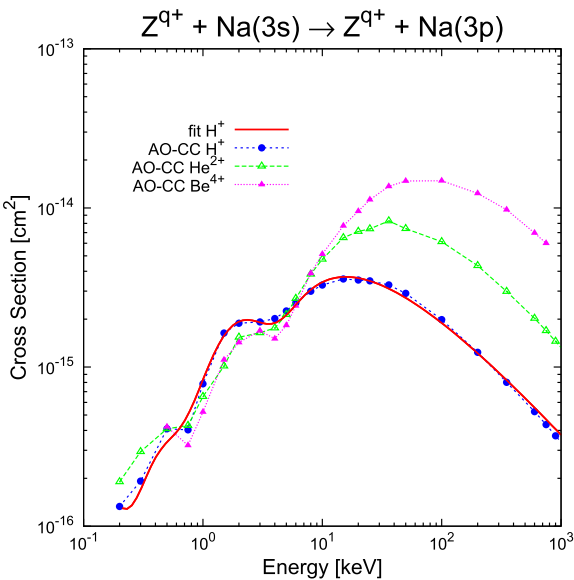


Fig. 7. Cross sections of collisions of Na with H^+ , He^{2+} , and Be^{4+} ions for the transition $Na(3s) \rightarrow Na(3p)$. The fit is for proton-impact excitation in terms of Eq. (7) and Table 3.

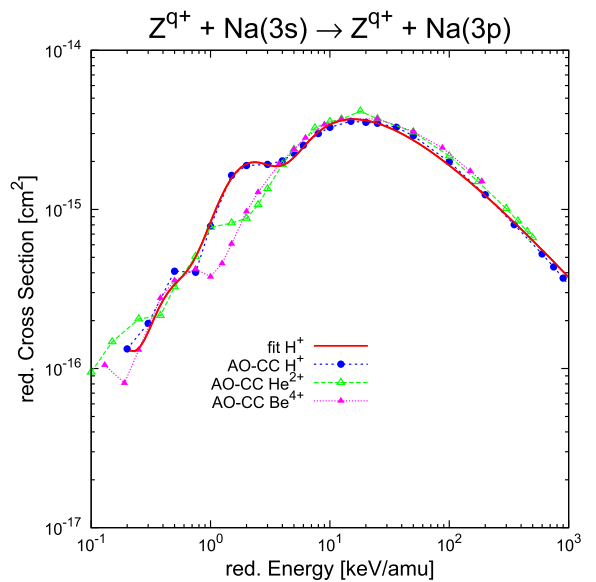


Fig. 8. Reduced cross sections σ/q of collisions of Na with H^+ , He^{2+} , and Be^{4+} ions for the transition $Na(3s) \rightarrow Na(3p)$. Reduced cross sections σ/q of collisions of Na with H^+ , He^{2+} , and Be^{4+} ions for the transition $Na(3s) \rightarrow Na(3p)$. For reduced energies $E/q > 3 \frac{\text{keV}}{\text{amu}}$, the reduced cross sections of He^{2+} and Be^{4+} follow the proton-impact cross section very well. The fit is for proton-impact excitation in terms of Eq. (7) and Table 3.

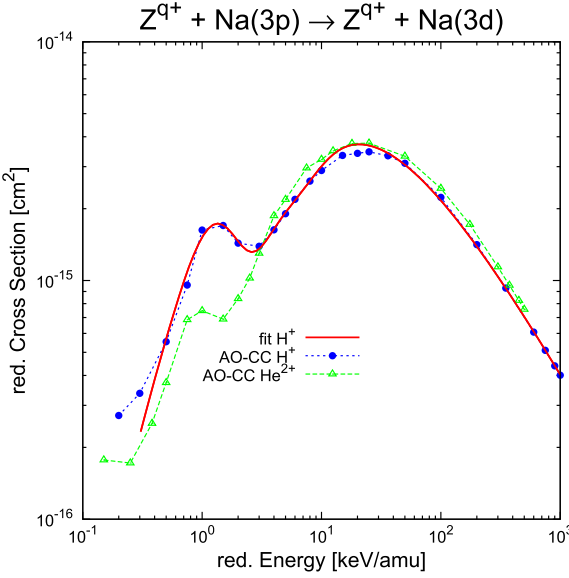


Fig. 9. Reduced cross sections σ/q of collisions of Na with H^+ and He^{2+} ions for the transition $\text{Na}(3p) \rightarrow \text{Na}(3d)$. The fit is for proton-impact excitation in terms of Eq. (7) and Table 3.

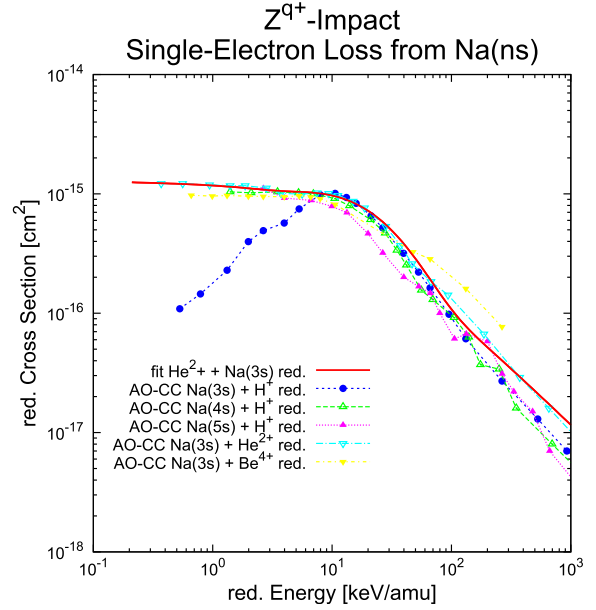


Fig. 11. Reduced cross sections of collisions of $\text{Na}(ns)$ with H^+ , He^{2+} , and Be^{4+} ions resulting in Na electron loss. Eq. (9) was fitted to the reduced He^{2+} cross section. For parameters, see Table H.

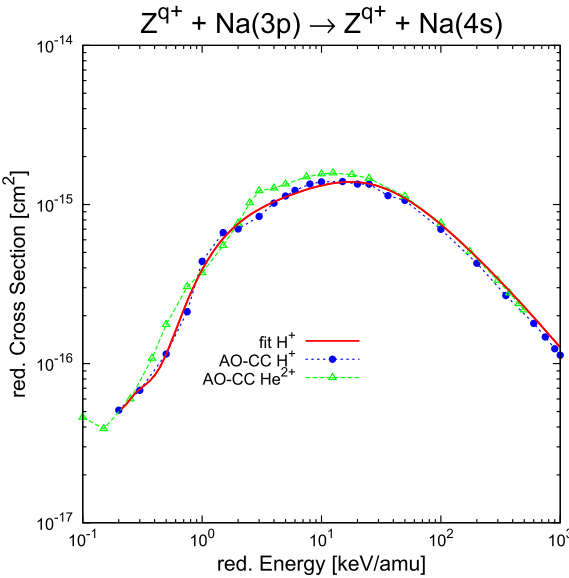


Fig. 10. Reduced cross sections σ/q of collisions of Na with H^+ , He^{2+} , ions for the transition $\text{Na}(3p) \rightarrow \text{Na}(4s)$. The fit is for proton-impact excitation in terms of Eq. (7) and Table 3.

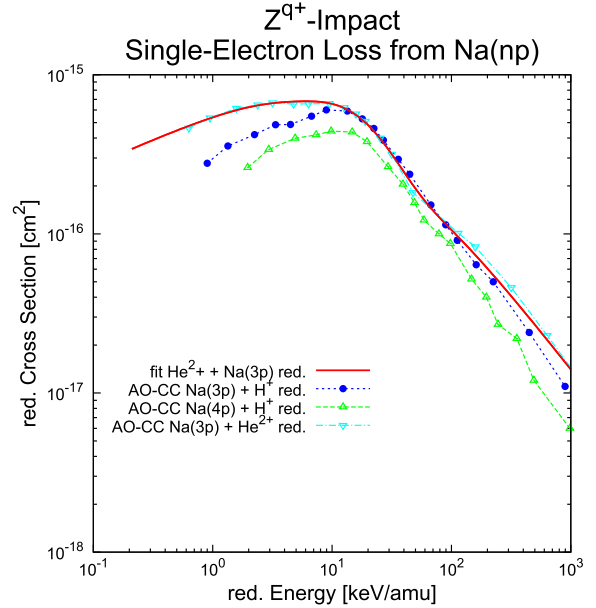


Fig. 12. Reduced cross sections of collisions of $\text{Na}(np)$ with H^+ and He^{2+} ions resulting in Na electron loss. Eq. (9) was fitted to the reduced He^{2+} cross section. For parameters, see Table H.

tems are close to resonance ($H^+ - \text{Na}(4s, 5s)$) or are quasi-resonant ($Z^{q+} - \text{Na}(ns)$). Therefore, the fitted (Eq. (9)) reduced He^{2+} ELOSS cross section represents a general curve from which cross sections for any projectile of higher q and initial $\text{Na}(ns)$ can be derived. In the case of initial $\text{Na}(np)$ the situation is similar and again the fit

to the He^{2+} data serve as the general curve from which all cross sections for higher charged projectiles can be derived. Table H shows the corresponding fit parameters. For even higher excited initial $\text{Na}(nl)$ the scaling relation (Eq. (11)) can be directly applied to the fit of $H^+ - \text{Na}(nl)$.

Table H

Fit parameters for reduced cross sections of He^{2+} impact of $\text{Na}(nl)$; $n = 3$

nl	E_{low}	A_1	A_2	A_3	A_4	A_5	A_6
3s	0.2	3.2558	16.009	4.03×10^{12}	3.7687	0.437	0.0167
3p	0.2	17.7447	22.2931	14.8373	0.3208	0.0791	-0.3255

Acknowledgments

This work, supported by the European Communities under the contract of Association between EURATOM and the Austrian Academy of Sciences, was carried out within the framework of the European Fusion Development Agreement. The views and opinions expressed herein do not necessarily reflect those of the European Commission. K.I. is a recipient of a DOC-fFORTE-fellowship of the Austrian Academy of Sciences at the Institut für Allgemeine Physik at Vienna University of Technology. This work was also supported by the Friedrich-Schiedel-Stiftung für Energietechnik. The work of I.B. was supported by the Australian Research Council, the Australian Partnership for Advanced Computing and its Western Australian node iVEC.

References

- [1] F. Aumayr, R. Schorn, M. Pöckl, J. Schweinzer, E. Wolfrum, K. McCormick, E. Hintz, HP. Winter, *J. Nucl. Mater.* 196–198 (1992) 928.
- [2] J. Schweinzer, E. Wolfrum, F. Aumayr, M. Pöckl, HP. Winter, R. Schorn, E. Hintz, A. Unterreiter, *Plasma Phys. Control. Fusion* 34 (1992) 1173.
- [3] E. Wolfrum, F. Aumayr, D. Wutte, HP. Winter, E. Hintz, D. Rusbüldt, R. Schorn, *Rev. Sci. Instrum.* 64 (1993) 2285.
- [4] R. Brandenburg, J. Schweinzer, S. Fiedler, F. Aumayr, HP. Winter, *Plasma Phys. Control. Fusion* 41 (1999) 471.
- [5] F. Aumayr, HP. Winter, *Ann. Phys.* 497 (1985) 228.
- [6] D. Wutte, R. Janev, F. Aumayr, M. Schneider, J. Schweinzer, J. Smith, HP. Winter, *At. Data Nucl. Data Tables* 65 (1997) 155.
- [7] J. Schweinzer, R. Brandenburg, I. Bray, R. Hoekstra, F. Aumayr, R. Janev, HP. Winter, *At. Data Nucl. Data Tables* 72 (1999) 239.
- [8] S. Fiedler, R. Brandenburg, J. Baldzuhn, K. McCormick, F. Aumayr, J. Schweinzer, HP. WinterW7-AS, ASDEX Upgrade team, *J. Nucl. Mater.* 266 (1999) 1279.
- [9] R. Schorn, E. Hintz, D. Rusbüldt, F. Aumayr, M. Schneider, E. Unterreiter, HP. Winter, *Appl. Phys. B* 52 (1991) 71.
- [10] R. Schorn, E. Wolfrum, F. Aumayr, E. Hintz, D. Rusbüldt, HP. Winter, *Nucl. Fusion* 32 (1992) 351.
- [11] E. Wolfrum, J. Schweinzer, M. Reich, L. Horton, C. Maggi, *Rev. Sci. Instrum.* 77 (2006) 033507.
- [12] I. Bray, A.T. Stelbovics, *Phys. Rev. A* 46 (1992) 6995.
- [13] I. Bray, *Phys. Rev. A* 49 (1994) 1066.
- [14] I. Bray, A. Stelbovics, *Phys. Rev. Lett.* 69 (1992) 53.
- [15] R. Brandenburg, J. Schweinzer, F. Aumayr, HP. Winter, *J. Phys. B: At. Mol. Phys.* 31 (1998) 2585.
- [16] W. Fritsch, C.D. Lin, *Phys. Rep.* 202 (1991) 1.
- [17] J. Schweinzer, D. Wutte, HP. Winter, *J. Phys. B: At. Mol. Phys.* 27 (1994) 137.
- [18] W.H. Press, Numerical Recipes in C—The Art of Scientific Computing, Cambridge University Press, Cambridge, MA, 1992 (Chapter 15.5), 681 pp..
- [19] T. Williams, C. Kelley, gnuplot—An Interactive Plotting Program, 2004.
- [20] W. Lotz, *Z. Phys.* 216 (1968) 241.
- [21] W. Lotz, *J. Opt. Soc. Am.* 58 (1968) 915.
- [22] K. Fujii, S. Srivastava, *J. Phys. B: At. Mol. Phys.* 28 (1995) L559.
- [23] D. Bates, G. Griffing, *Proc. Phys. Soc. London* 66 (1953) 961.
- [24] R. Janev, L. Presnyakov, *J. Phys. B: At. Mol. Phys.* 13 (1980) 4233.
- [25] R. Janev, *Phys. Lett. A* 160 (1991) 67.
- [26] S. Buckman, P. Teubner, *J. Phys. B: At. Mol. Phys.* 12 (1979) 1741.
- [27] J. Mitroy, I. McCarthy, A. Selbovics, *J. Phys. B: At. Mol. Phys.* 20 (1987) 4827.
- [28] E. Enemark, A. Gallagher, *Phys. Rev. A* 6 (1972) 192.
- [29] G. Gould, Ph.D. Thesis, University of New South Wales, 1970.
- [30] D. Moores, D. Norcross, *J. Phys. B: At. Mol. Phys.* 5 (1972) 1482.
- [31] E. Karule, *J. Phys. B: At. Mol. Phys.* 3 (1970) 860.
- [32] Y.-K. Kim, *Phys. Rev. A* 64 (2001) 032713.
- [33] J. Phelps, C. Lin, *Phys. Rev. A* 24 (1981) 1299.
- [34] S. Srivastava, L. Vušković, *J. Phys. B: At. Mol. Phys.* 13 (1980) 2633.
- [35] I. Zapatoschnyi, E. Postoi, I. Aleksakhin, *Sov. Phys. JETP* 41 (1976) 865.
- [36] P. Ganas, *J. Appl. Phys.* 57 (1985) 154.
- [37] B. Stumpf, A. Gallagher, *Phys. Rev. A* 32 (1985) 3344.
- [38] S. Verma, R. Srivastava, *J. Phys. B: At. Mol. Phys.* 29 (1996) 3215.
- [39] D.R. Bates, A.H. Boyd, S.S. Prasad, *Proc. Phys. Soc. London* 85 (1965) 1121.
- [40] K. Omidvar, H. Kyle, E. Sullivan, *Phys. Rev. A* 5 (1972) 1174.
- [41] A. Johnston, P. Burrow, *Phys. Rev. A* 51 (1995) R1735.
- [42] E. McGuire, *Phys. Rev. A* 3 (1971) 267.
- [43] E. McGuire, *J. Phys. B: At. Mol. Phys.* 30 (1997) 1563.
- [44] N. Rakstikas, A. Kulplauskiene, *Phys. Scripta* 64 (2001) 230.
- [45] W.S. Tan, Z. Shi, C.H. Ying, L. Vušković, *Phys. Rev. A* 54 (1996) R3710.
- [46] I. Zapatoschnyi, I. Aleksakhin, *Zh. Eksp. Teor. Fiz.* 55 (1968) 76.
- [47] J. Allen, L. Anderson, C. Lin, *Phys. Rev. A* 37 (1988) 349.
- [48] C. Theodosiou, *Phys. Rev. A* 38 (1988) 4923.
- [49] F. Aumayr, G. Lakits, HP. Winter, *J. Phys. B: At. Mol. Phys.* 20 (1987) 2025.
- [50] W. Fritsch, *Phys. Rev. A* 35 (1987) 2342.
- [51] R. Shingal, B. Bransden, *J. Phys. B: At. Mol. Phys.* 20 (1987) 4815.
- [52] A. Howald, L. Anderson, C. Lin, *Phys. Rev. Lett.* 51 (1983) 2029.
- [53] A. Jain, T. Winter, *Phys. Rev. A* 51 (1995) 2963.
- [54] W. Jitschin, S. Osimitsh, D. Mueller, H. Reihl, R.J. Allan, O. Schöller, H. Lutz, *J. Phys. B: At. Mol. Phys.* 19 (1986) 2299.
- [55] V. Lavrov, R. Lomsadze, Abstracts of Contributed Papers, 13th Intl. Conf. on Physics of Electronic and Atomics Collisions, Berlin, North-Holland, Amsterdam, 1983, 610 pp.
- [56] C. Theodosiou, *Phys. Rev. A* 36 (5) (1987) 2067.
- [57] R. Shingal, B. Bransden, A. Ermolaev, D. Flower, C. Newby, C. Noble, *J. Phys. B: At. Mol. Phys.* 19 (1986) 309.
- [58] C. Stary, H. Lüdde, R. Dreizler, *J. Phys. B: At. Mol. Phys.* 23 (1990) 263.
- [59] C. Anderson, A. Howald, L. Anderson, *Nucl. Instrum. Methods* 165 (1979) 583.
- [60] L. Anderson, J. Allen, C. Lin, R. Miers, in: Proc. 14th Int. Conf. on Physics of Electronic and Atomic Collisions, North Holland, Amsterdam, 1985, 385 pp.
- [61] R. DuBois, L. Toburen, *Phys. Rev. A* 31 (1985) 3603.
- [62] R. DuBois, *Phys. Rev. A* 34 (1986) 2738.
- [63] F. Ebel, E. Salzborn, *J. Phys. B: At. Mol. Phys.* 20 (1987) 4531.
- [64] A. Ermolaev, *J. Phys. B: At. Mol. Phys.* 17 (1984) 1069.
- [65] W. Fritsch, *Phys. Rev. A* 30 (1984) 1135.
- [66] M. Kimura, R. Olson, J. Pascale, *Phys. Rev. A* 26 (1982) 3113.
- [67] A. Perumal, D. Tripathi, *J. Phys. Soc. Jpn.* 66 (1997) 3783.
- [68] F. Sattin, *Phys. Rev. A* 64 (2001) 034704.
- [69] J.W. Thomsen, N. Andersen, D. Dowek, J.C. Houwer, J.H.V. Lauritsen, U. Müller, J.O.P. Pedersen, J. Salgado, A. Svensson, *Z. Phys. D: At. Mol. Clusters* 37 (1996) 133.
- [70] D. Bates, A. Kingston, Advances in Atomic and Molecular Physics, vol. 6, Academic Press, New York, 1970, 269 pp.
- [71] C. Lundy, R. Olson, *J. Phys. B: At. Mol. Phys.* 29 (1996) 1723.
- [72] B. O'Hare, R. McCullough, H. Gilbody, *J. Phys. B: At. Mol. Phys.* 8 (1975) 2968.

Explanation of Tables

Table 1. Fit parameters for electron-impact target-excitation cross sections of Na($nl \rightarrow n'l'$); $n, n' = 3-5$

$nl \rightarrow n'l'$ Initial–final states of the Na atom
 ΔE Excitation energy of the EXC process in eV
 A_1, \dots, A_7 Fit parameters as in Eq. (1)

Table 2. Fit parameters for electron-impact target-ionization cross sections of Na(nl); $n = 3-5$

nl Initial state of the Na atom
 I_{nl} Ionization energy in eV
 A_1, \dots, A_6 Fit parameters as in Eq. (2)

Table 3. Fit parameters for proton-impact target-excitation cross sections of Na($nl \rightarrow n'l'$); $n, n' = 3-5$

$nl \rightarrow n'l'$ Initial–final states of the Na atom
 A_1, \dots, A_{12} Fit parameters as in Eq. (7)

Table 4. Fit parameters for proton-impact target-electron-loss cross sections of Na(nl); $n = 3-5$

nl Initial state of the Na atom
 A_1, \dots, A_6 Fit parameters as in Eq. (9)

Explanation of Graphs

Graphs 1–28. **Electron-impact target-excitation cross sections of Na($nl \rightarrow n'l'$); $n, n' = 3–5$**
 $nl \rightarrow n'l'$ Initial–final states of the Na atom.

Graphs 29–36. **Electron-impact target-ionization cross sections from Na(nl); $n = 3–5$**
 nl Initial state of the Na atom

Graphs 37–64. **Proton-impact target-excitation cross sections from Na($nl \rightarrow n'l'$); $n, n' = 3–5$**
 $nl \rightarrow n'l'$ Initial–final states of the Na atom

Graphs 65–72. **Proton-impact target-electron-loss cross sections from Na(nl); $n = 3–5$**
 nl Initial state of the Na atom

Table 1Fit parameters for electron-impact target excitation cross section of Na($nl \rightarrow n'l'$); $n, n' = 3\text{--}5$. See page 991 for Explanation of Tables

$nl \rightarrow n'l'$	ΔE	A_1	A_2	A_3	A_4	A_5	A_6	A_7
3s → 3p	2.09937	-23.3231	38.358	-5.70599	-3.4816	27.1453	0.453874	14.7003
3s → 3d	3.61642	54.0317	-27.3057	-28.6423	35.1405	-0.288761	0.381653	1.04435
3s → 4s	3.19192	2.51105	-10.8455	21.3071	-13.2455	0	0.58	11.3285
3s → 4p	3.75248	10.5845	-44.94	74.7574	-40.3895	2.12788	5.9750×10^{-3}	1.67677
3s → 4d	4.28447	6.22968	10.1143	-34.6957	32.5314	0.13928	1.08379	2.04554
3s → 4f	4.28855	0.753717	13.9336	-35.7825	31.9556	0.0297361	0.814152	1.67582
3s → 5s	4.11711	18.3199	-52.2671	52.2258	4.31253	0.877115	0.504837	0.253928
3p → 3d	1.51705	-274.892	380.104	-38.007	-51.4476	208.52	3.6757×10^{-3}	2.21269
3p → 4s	1.09255	-8.15967	19.8158	-29.2698	28.5195	5.47456	0.948679	24.7919
3p → 4p	1.65311	4.87684	-11.1746	16.1142	-6.00012	0.100725	0.791831	14.9378
3p → 4d	2.1851	-2.1686	-36.4101	86.9806	-38.8431	16.307	0.06977	2.2177
3p → 4f	2.18918	2.3848	3.1897	-19.6921	21.5142	-0.0105359	0.839963	15.4706
3p → 5s	2.01774	1.2911	-14.0441	29.5538	-16.5211	1.56757	0.02045	3.2114
3d → 4p	0.13606	-4.17001	-10.1151	137.921	-59.7171	11.0426	3.96822	60.5028
3d → 4d	0.668046	4.64022	15.006	-147.95	270.543	0.176582	2.6348	46.0857
3d → 4f	0.672127	-1.6638×10^3	1.5201×10^3	334.707	4.8787×10^3	1.0803×10^3	2.38353	1.18888
3d → 5s	0.50069	0.354729	11.0975	-38.9064	67.6696	0.0158897	2.77575	50.1735
4s → 3d	0.4245	9.83953	-61.7689	180.035	-89.1436	0.208417	2.5022	49.9816
4s → 4p	0.56056	-766.196	1.45×10^3	0	0	539.17	3.36726	4.00164
4s → 4d	1.09255	-1.05183	-73.0017	371.593	-654.485	-0.128653	4.49224	-47.2604
4s → 4f	1.09663	-3.00114	-58.8159	333.103	-675.733	-0.11054	4.49224	-36.4141
4s → 5s	0.92519	7.40763	-52.1312	116.889	-54.6344	1.06354	1.63344	10.6933
4p → 4d	0.531986	-2.1967×10^3	3.4305×10^5	-1.8810×10^6	6.1742×10^5	-2.2207×10^4	9.11098	-0.0493211
4p → 4f	0.536067	411.469	-2.3604×10^3	4.932×10^3	-2.3127×10^3	14.533	1.80954	1.5026
4p → 5s	0.36463	-6.70865	-211.981	1.3883×10^3	-522.46	16.0299	8.01689	36.2413
4d → 4f ^a	4.08×10^{-3}	-335.85	-1.7174×10^3	411.336	-2.99991	330.533	3.3763×10^{-5}	11.1878
5s → 4d	0.167356	4.25353	-45.5338	562.593	-151.995	3.0812×10^{-3}	16.3001	560.193
5s → 4f	0.171437	12.4203	-126.653	615.687	-306.243	-0.041334	4.36124	34.695

^a The fit parameters for 4d → 4f are only valid above 0.2 eV.

Table 2

Fit parameters for electron-impact target ionization cross sections of the valence electron in Na(nl); $n = 3–5$. See page 991 for Explanation of Tables

nl	I_{nl}	E_{low}	A_1	A_2	A_3	A_4	A_5	A_6	A_7
3s	5.13891	5.2	0	66.4483	24.5645	101.03	-5.0082	0	4.37×10^{-3}
3p	3.03954	3.2	20.8332	-13.1449	-19.4089	33.258	0.542801	-56.3793	0.0379105
3d	1.52249	2.08	-105.202	-21.5898	485.919	-337.711	0.369663	331.13	0.0351848
4s	1.94699	2.5	-0.729955	-0.0916904	3.32036	-2.34172	9.0515×10^{-5}	2.25425	3.72267
4p	1.38643	1.9	-28.9039	-6.49469	130.161	-92.2872	0.19249	91.127	0.176319
4d	0.850363	1.7	0.0711827	7.87424	-17.7004	8.79277	-0.0200515	-5.48488	-0.446075
4f	0.850363	1.3	1.8088	2.13387	-12.4468	8.35135	-6.259×10^{-3}	-6.66904	-2.2193
5s	1.0218	1.5	-3.83331	-2.65103	21.742	-14.8678	2.5528×10^{-3}	13.1159	1.28082

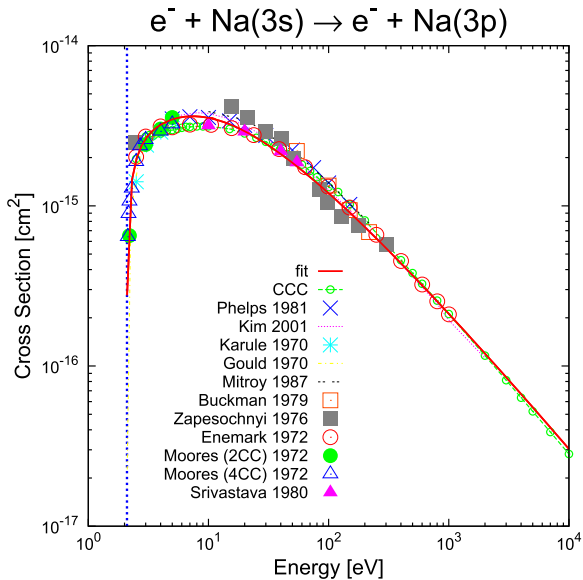
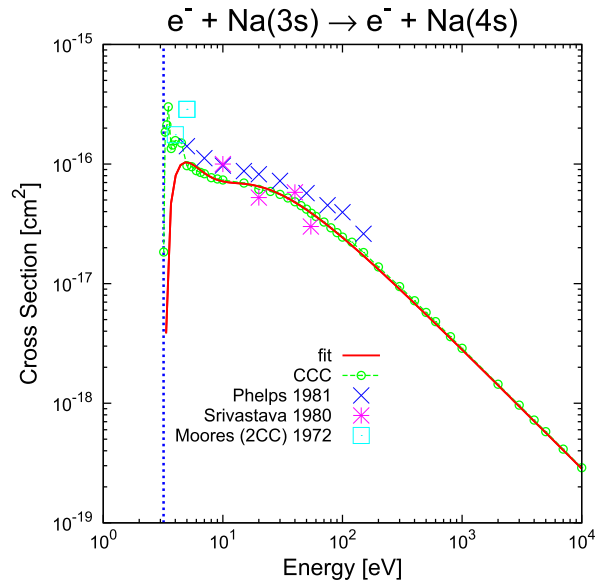
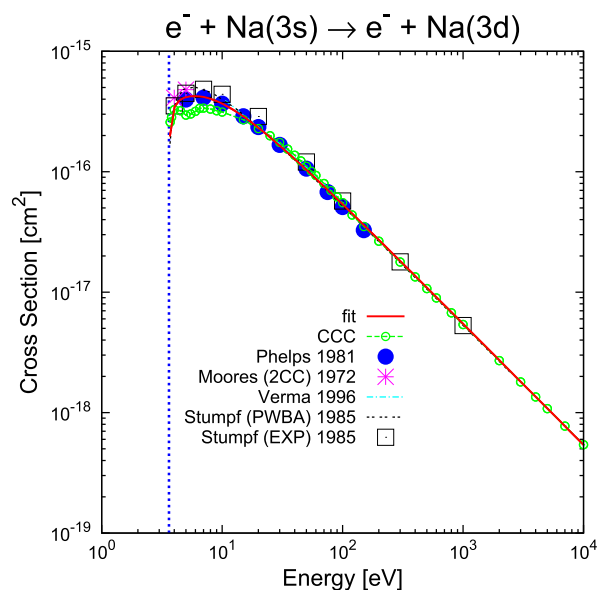
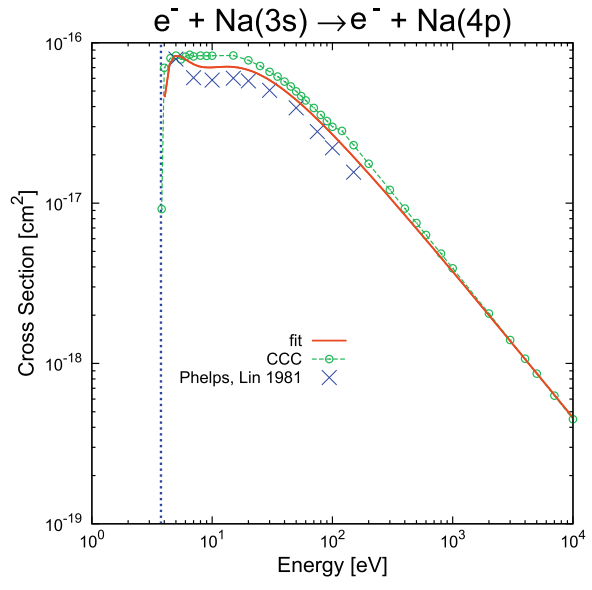
Fits containing inner-shell ionization can be obtained using Eqs. (4) and (3) together with Table D.

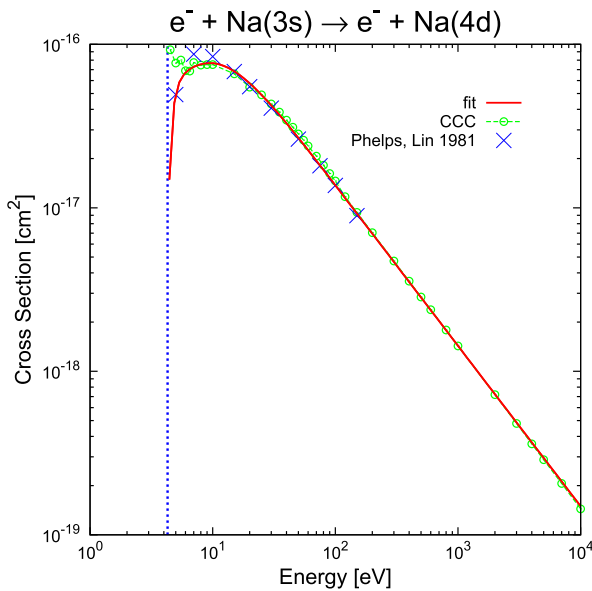
Table 3Fit parameters for proton-impact target excitation cross sections of Na($nl \rightarrow n'l'$); $n, n' = 3\text{--}5$. See page 991 for Explanation of Tables

$nl \rightarrow n'l'$	E_{low}	A_1	A_2	A_3	A_4	A_5	A_6	A_7	A_8	A_9	A_{10}	A_{11}	A_{12}
3s → 3p	0.2	899.91	0.813273	0.172984	0.171027	1.33781	-1.97329	-9.90738	1.82931	20.1605	0.899862	0.934209	-0.012689
3s → 3d	0.2	2.35787	16.0799	1.661×10^8	1.75626	1.88912	-3.32454	9.56875	14.1112	0.0318923	1.56873	1	9.13887
3s → 4s	0.2	0.5291	11.1454	13.8	2.21	0.9258	-2.8909	-6.0985	4.29572	2.6×10^{-3}	2.1235	1.4632	93.1684
3s → 4p	0.3	12.287	1.00965	0.19894	-3.3202	4.7024	-6.149	69.9622	30.4996	3.1234	1.48366	1.38235	-0.32704
3s → 4d	1	0.09605	35.1151	0	6.5924	2.4005	-5.09985	21.6803	7.40333	2.7×10^{-3}	1.91665	1	272.253
3s → 4f	1	0.4652	44.0372	0	1.51204	2.38218	-5.305	178.707	27.0857	0.0628	2.30125	1.0×10^{-10}	29.7278
3s → 5s	0.6	21.912	67.9026	2.72934	3.5101×10^{-3}	0.941943	-3.9001	-43.6875	68.1887	1.82419	0.967314	6.44834	22.6012
3p → 3d	0.3	445.154	9.8646	0	0.0851	0.8208	-2.1403	-6.61	7.0552	0.2111	1.0887	1	26.1162
3p → 4s	0.2	875.942	0.0845244	3.2671	1.4616	0.12061	1.42592	-95.267	-0.041652	13.4883	0.92967	0.126126	4.83299
3p → 4p	0.3	13.2437	4.764	2.91617	1.44602	2.30177	-1.72801	34.7144	27.6903	0.19179	1.8542	0.525469	3.12512
3p → 4d	0.2	795.051	4.7911	3.2671	1.7546×10^{-3}	0.265715	-1.10414	-238.849	4.67249	6.89654	0.97723	-0.0730905	32.9442
3p → 4f	0.5	17.6253	9.36216	0	0.892868	7.8587×10^{-3}	0.782358	-6.63413	-0.0354364	7.58916	1.01267	1	4.62623
3p → 5s	0.5	170.3862	8.2541	-3.7×10^{-7}	200.96	11.083	-10.1593	1.1126	45.571	13.3755	0.841	0.591	0.6408
3d → 4p	1	301.658	30.0346	0	35.9391	4.67224	-0.758748	39.6619	1.22105	3.74937	0.881504	2.8484×10^{-7}	24.8598
3d → 4d	0.2	30.3405	6.373	0	0.2148	0.2718	-1.382	2.0156	0.4264	0.8904	2.6894	1	15.5586
3d → 4f	0.2	0.8662	12.0268	1.2596	-1.7409	0.0960	-1.0409	7.8386	0.3032	0.0419	0.7881	1.0006	525.2286
3d → 5s	0.3	1.97042	2.82693	0	36.1299	8.32895	-0.842273	22.1788	0.981295	0.077633	1.8594	1	26.1051
4s → 3d	0.2	76.102	0.108	1.4×10^3	4.79189	27.7	-45.7225	74.7606	1.8727	7.4108	1.094	-41.05	-4.97677
4s → 4p	0.7	3.0×10^3	0.181647	0.0152269	-1.00172	0.264541	0.553659	67.7319	30.4687	17.8543	0.984028	1.78496	0.348832
4s → 4d	0.3	12.2821	7.48675	0	41.5655	2.9866	-2.8764	47.503	67.1931	-0.91548	1.1443	1	100.0
4s → 4f	0.2	18.126	7.2308	0	0.3843	1.20817	-4.77267	1.0506	0.2524	1.1×10^{-3}	2.35044	1	13.724
4s → 5s	1	4.57798	73.0856	11.2459	55.6678	3.64108	1.22198	0.955863	0.0178534	3.9414×10^{-4}	1.95208	-0.55916	61.0529
4p → 4d	0.2	1.5105×10^3	41.0849	1.13114	5.48059	6.99795	-2.70534	0.0721157	1.14453	4.4491×10^{-4}	2.07563	3.00072	2.48347
4p → 4f	0.2	98.1211	5.2274	0	0.1986	0.9862	-3.3092	0.5538	0.09157	0.0539	1.0939	1	9.278
4p → 5s	0.2	695.167	0.379397	1.2862×10^{-3}	-0.0266469	4.46338	-12.1889	0.276855	2.18819	0.0374898	0.954608	1.03331	-1.3017×10^{-3}
4d → 4f	0.4	2.0×10^3	28.7819	0	35.9994	2.90774	-0.0355274	39.7245	0.089685	1.96664	0.943349	1.1334×10^{-8}	23.3783
5s → 4d	0.4	352.156	10.148	0	177.117	6.12077	-3.60091	283.157	4.75692	5.15505	2.46864	8.1046×10^{-4}	20.1594
5s → 4f	0.4	50.441	12.0566	0	-2.32538	0.333314	-0.669005	3.51249	-0.454977	0.0406219	1.83821	1.71289	14.6884

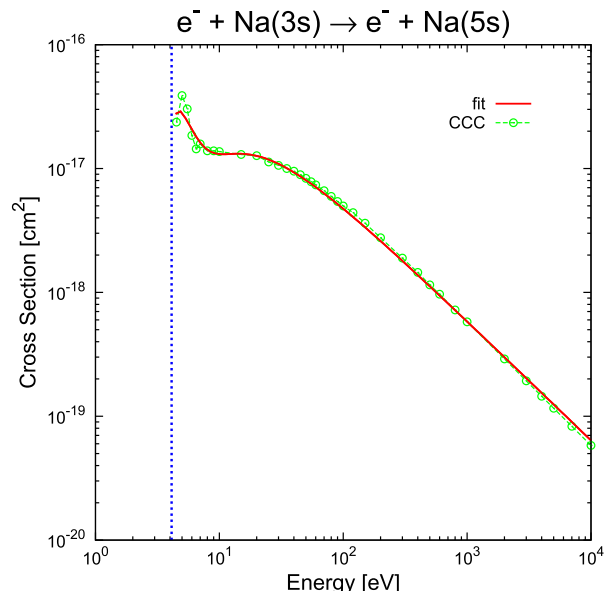
Table 4Fit parameters for proton-impact target electron loss from Na(nl); $n = 3\text{--}5$. See page 991 for Explanation of Tables

nl	E_{low}	A_1	A_2	A_3	A_4	A_5	A_6
3s	0.2	11.319	2.51212	1.0×10^5	2.26648	0.172847	-0.73075
3p	0.2	27.8562	1.5103	5.72×10^4	1.86786	0.0564	0.1081
3d	0.2	81.6464	1.4629	275.929	6.35454	0.372612	-0.0253238
4s	0.2	14.5812	1.0669	5.16×10^{13}	27.661	0.249027	0.159263
4p	0.2	31.4476	1.3675	3.1062×10^9	17.0752	0.665415	-0.369477
4d	0.2	66.0274	0.259161	4.8614×10^6	942.831	8.1801	-12.8437
4f	0.2	76.1757	0.21478	131.206	20.4186	0.892532	-0.184057
5s	0.2	27.7031	0.135768	2.0126×10^{12}	1.260×10^3	4.14424	-3.75084

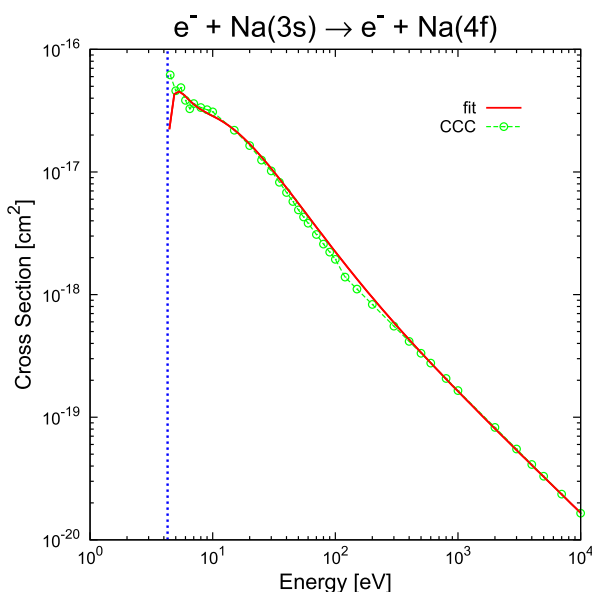
**Graph 1.****Graph 3.****Graph 2.****Graph 4.**



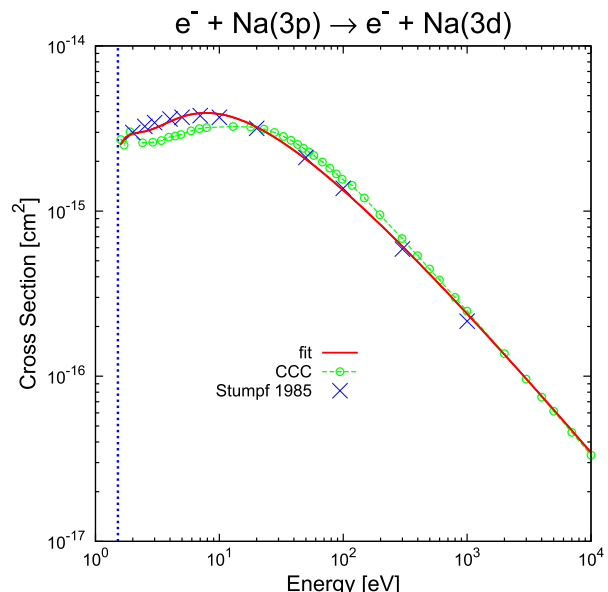
Graph 5.



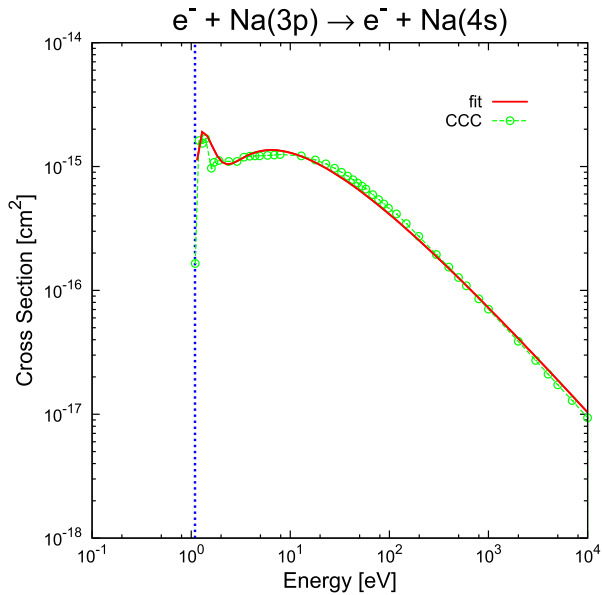
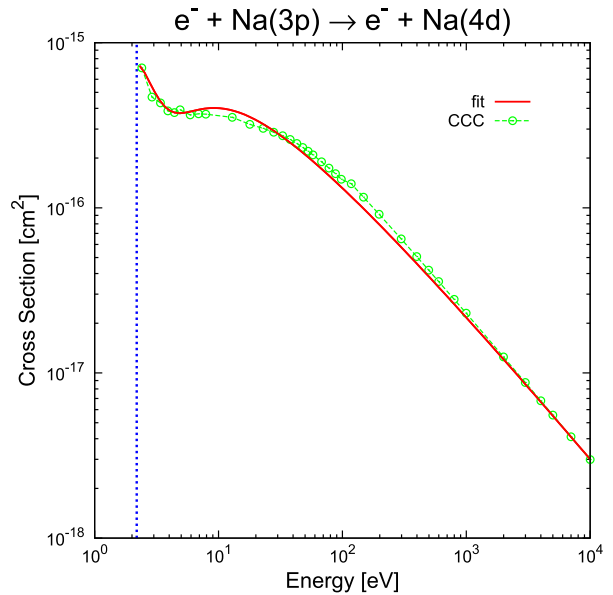
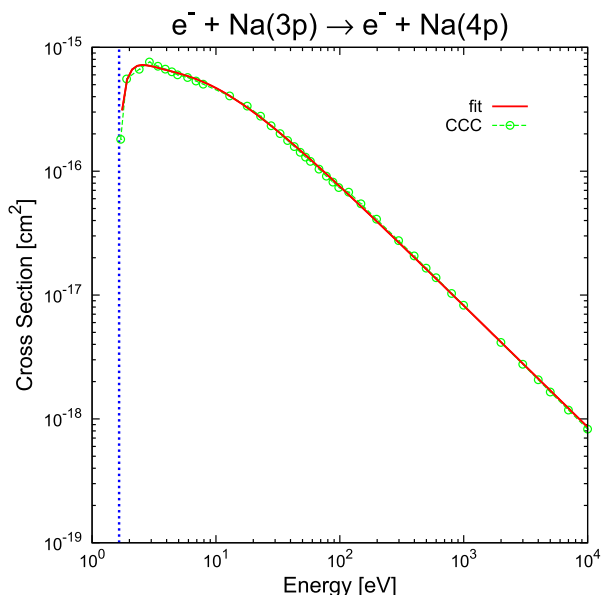
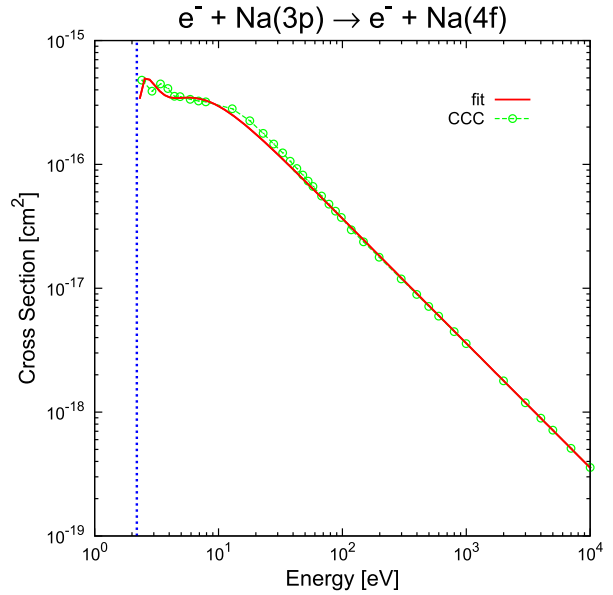
Graph 7.

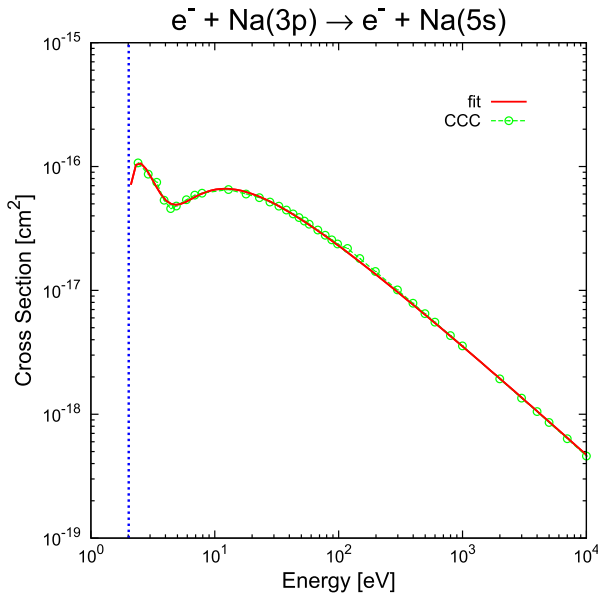


Graph 6.

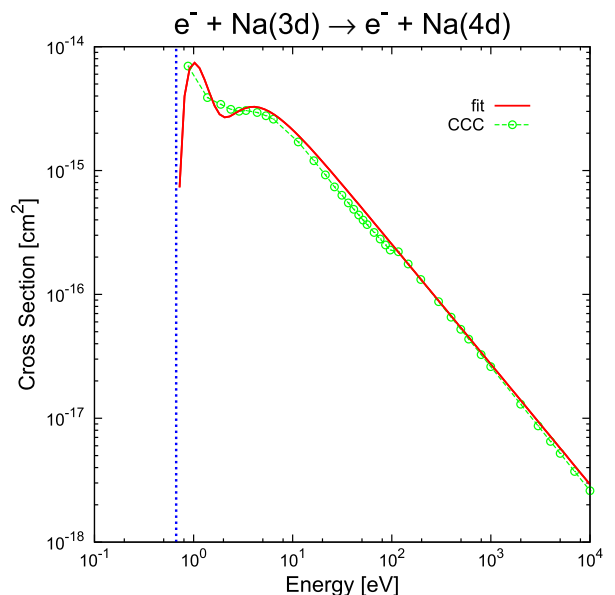


Graph 8.

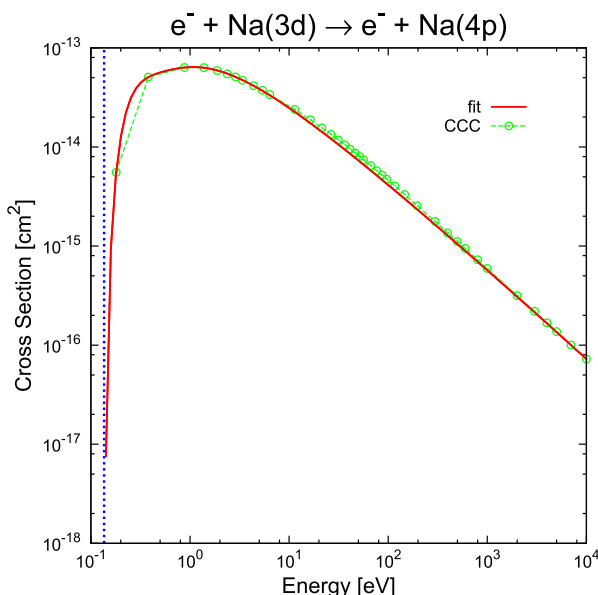
**Graph 9.****Graph 11.****Graph 10.****Graph 12.**



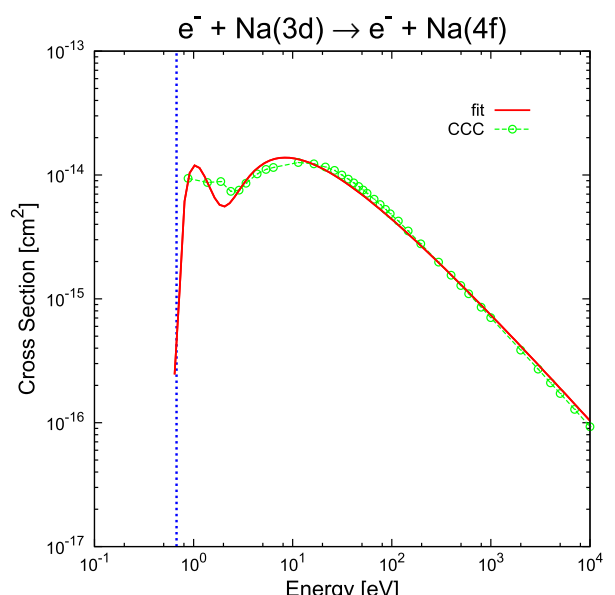
Graph 13.



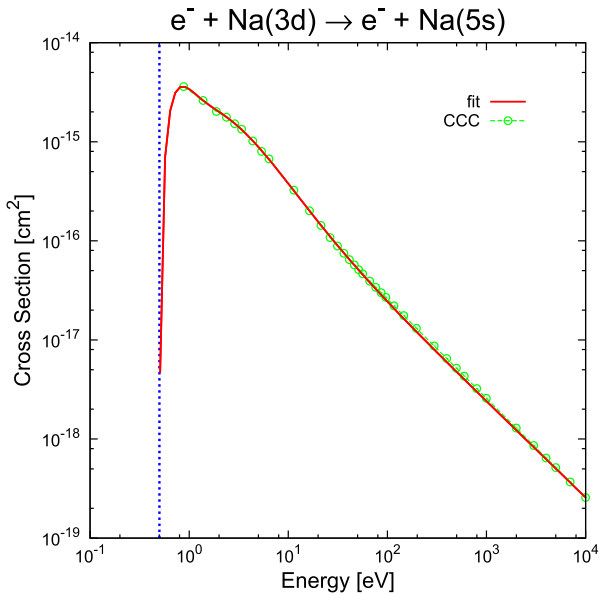
Graph 15.



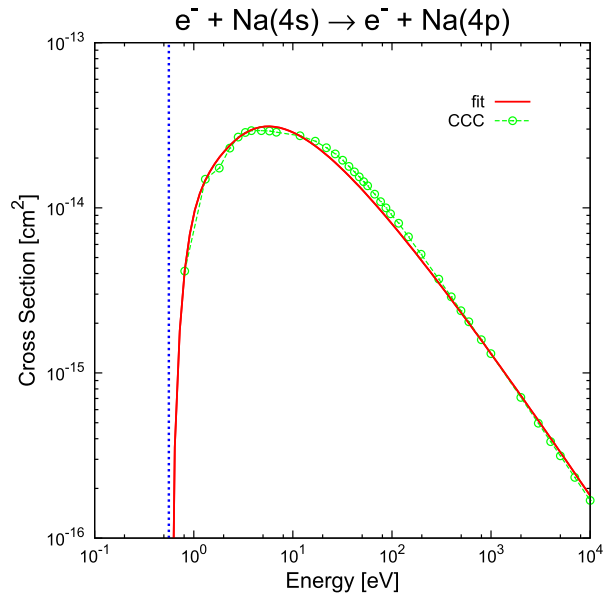
Graph 14.



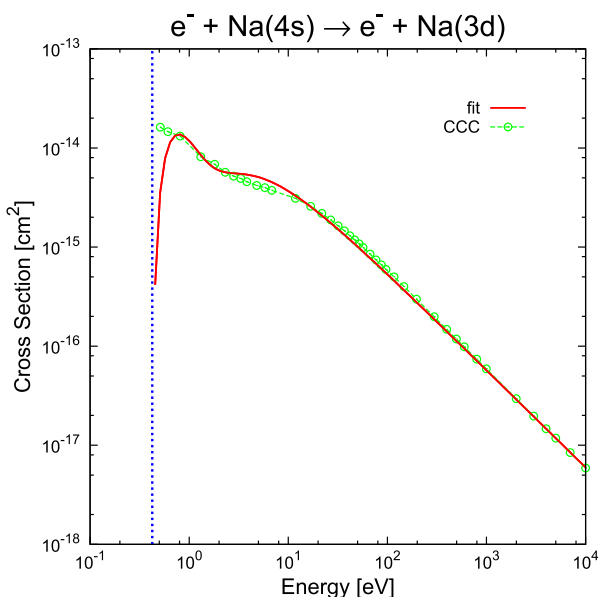
Graph 16.



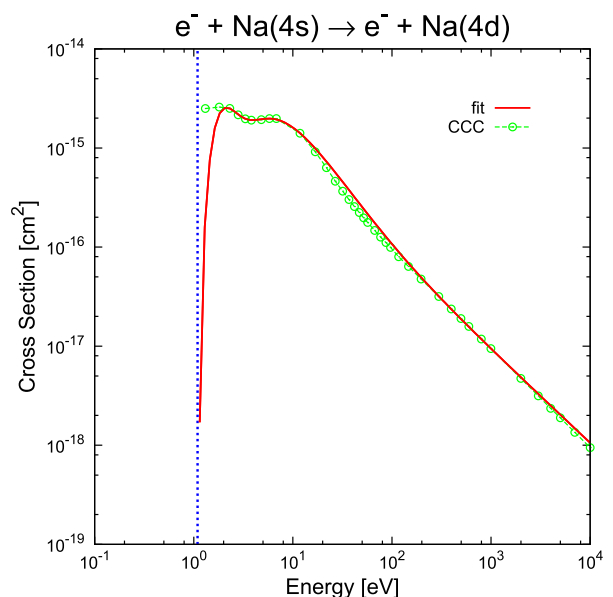
Graph 17.



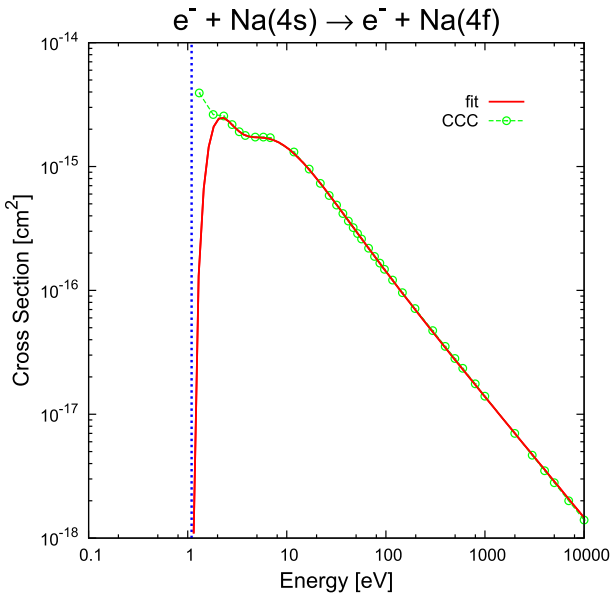
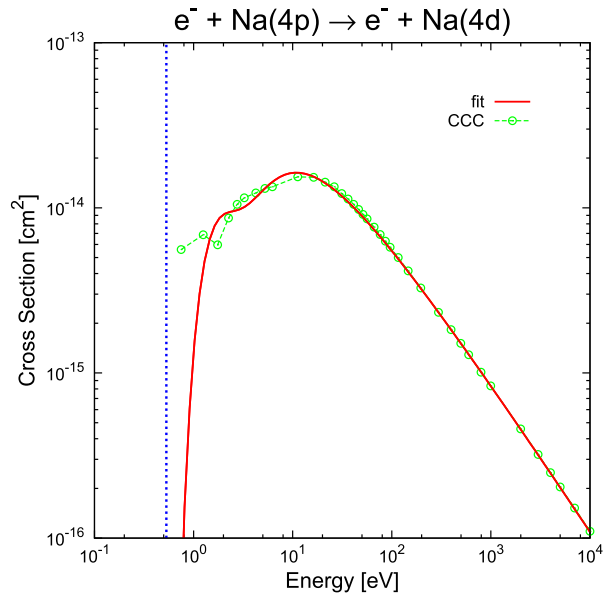
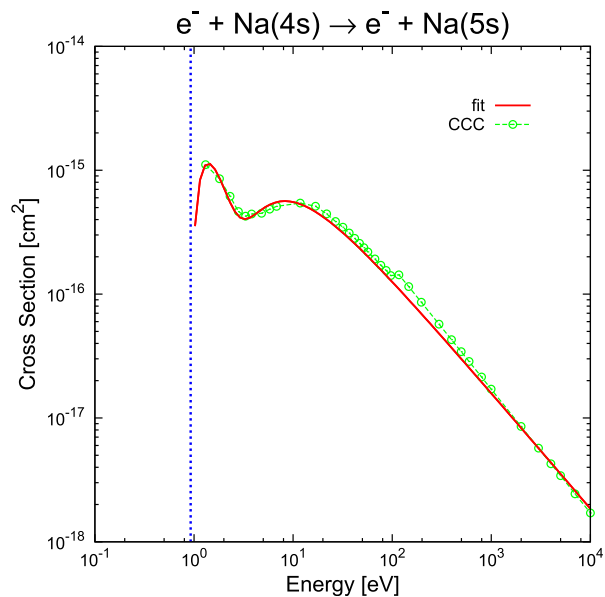
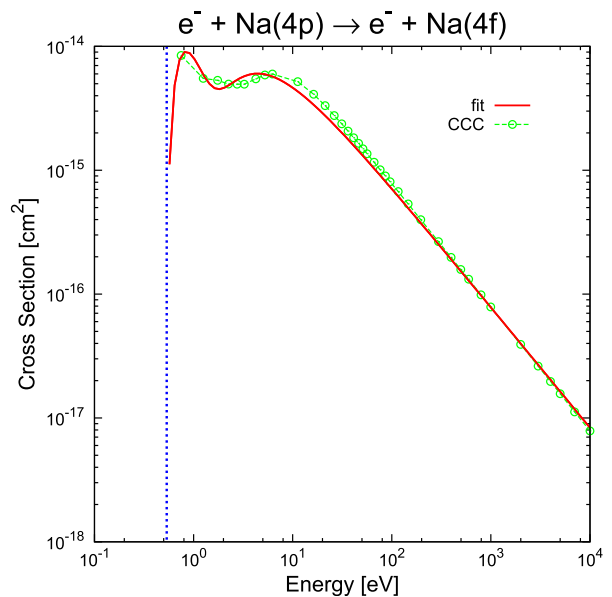
Graph 19.

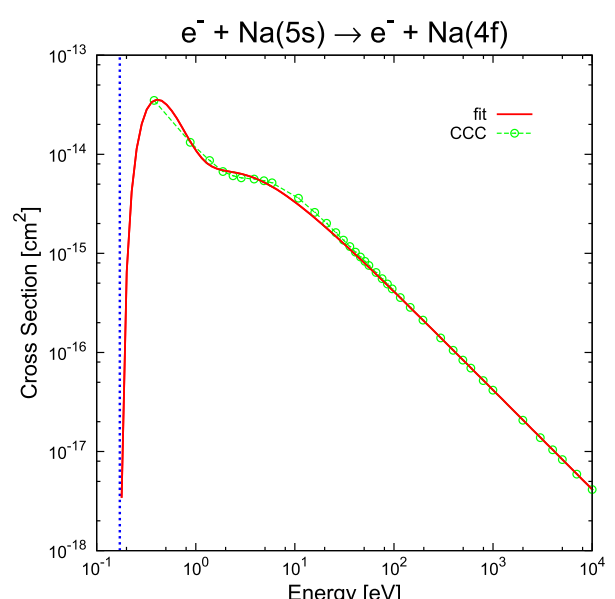
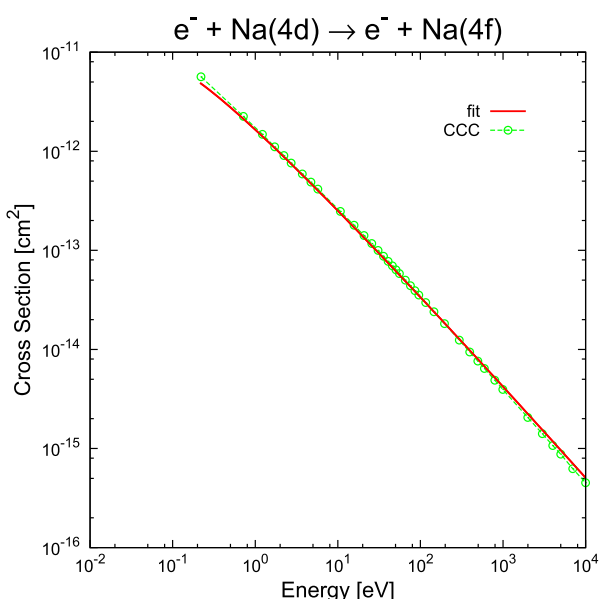
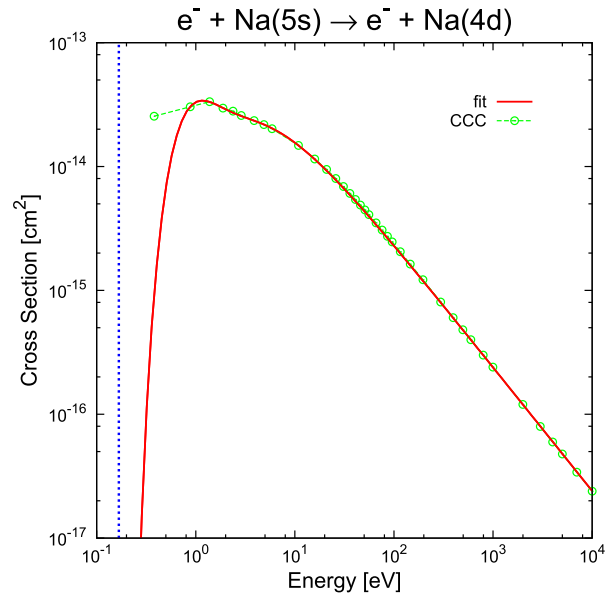
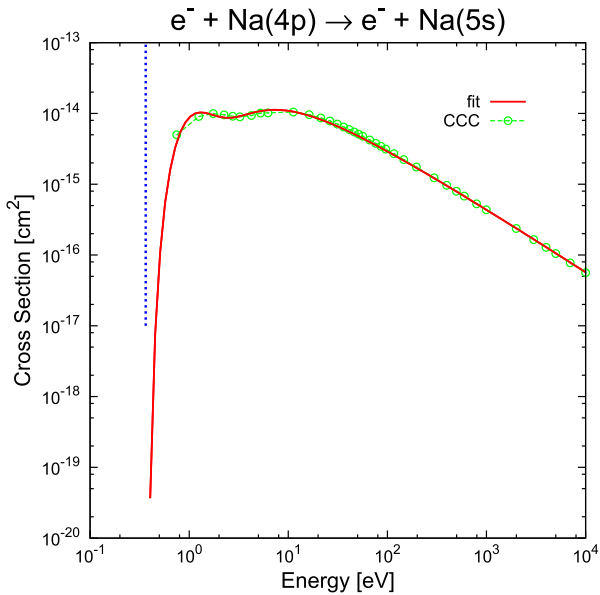


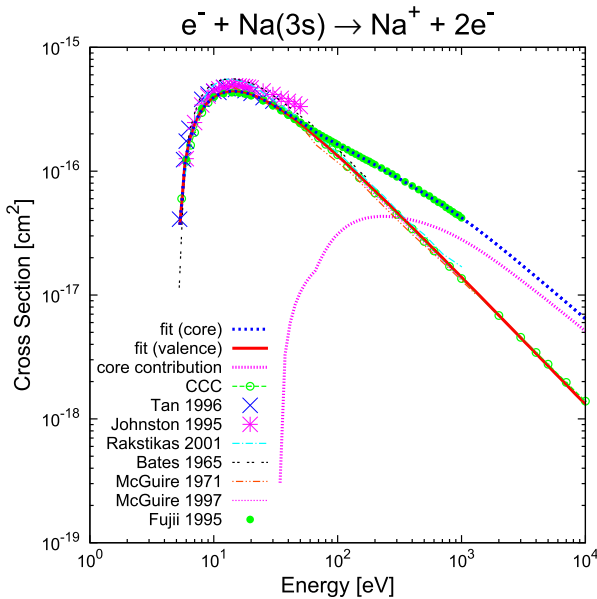
Graph 18.



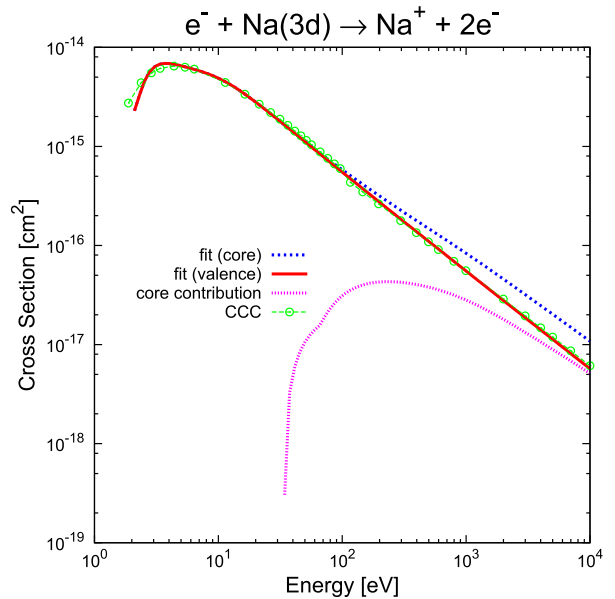
Graph 20.

**Graph 21.****Graph 23.****Graph 22.****Graph 24.**

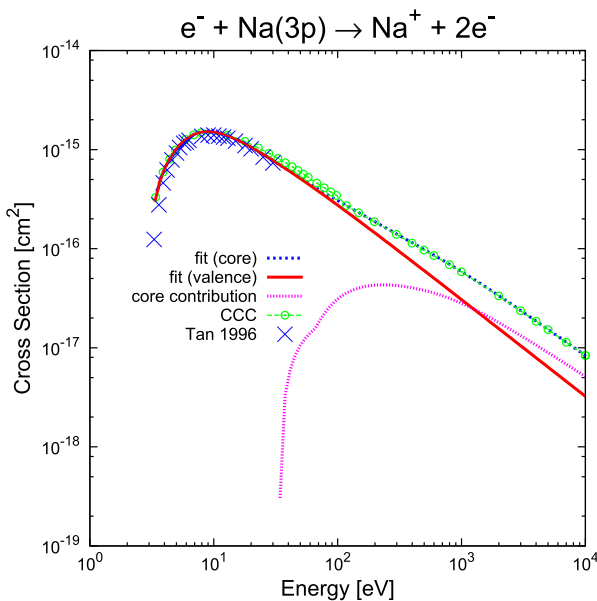




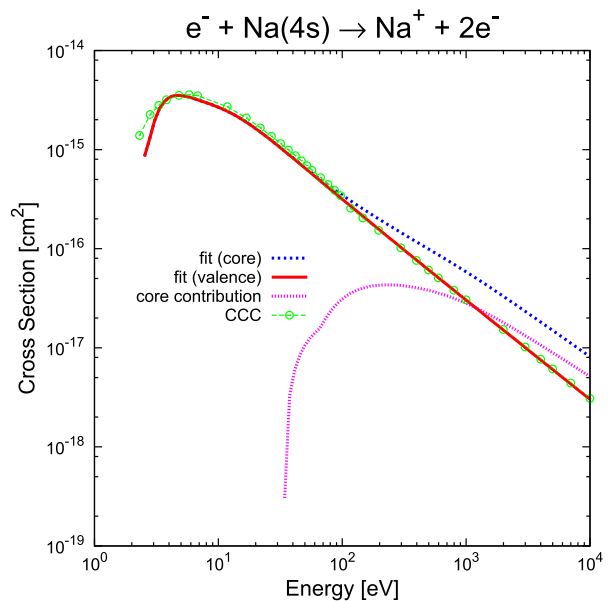
Graph 29.



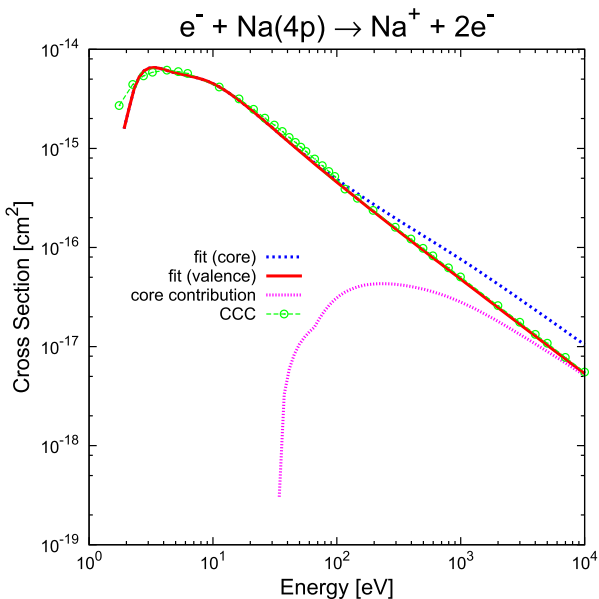
Graph 31.



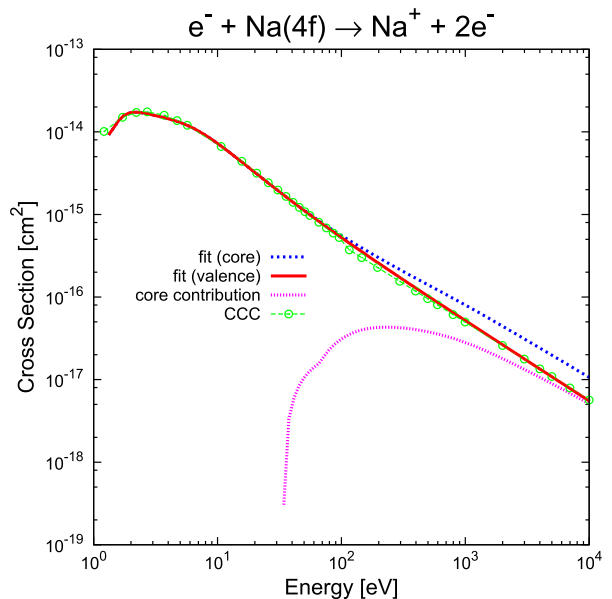
Graph 30.



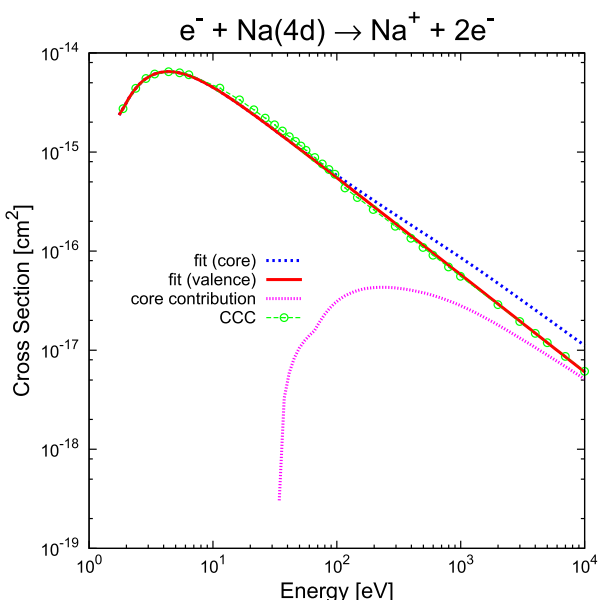
Graph 32.



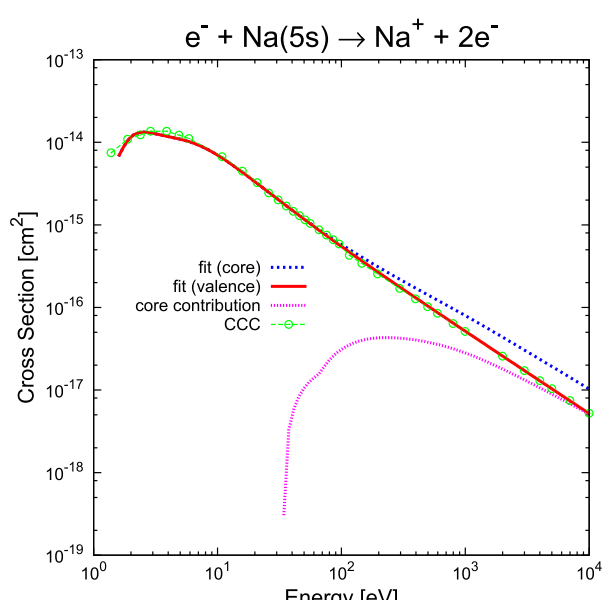
Graph 33.



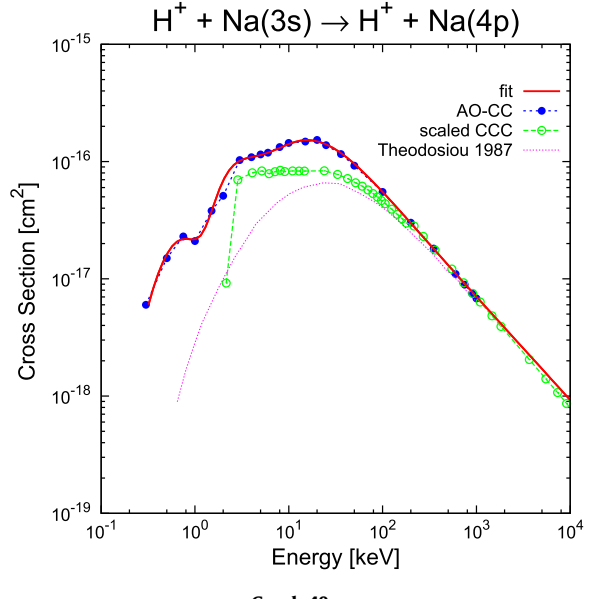
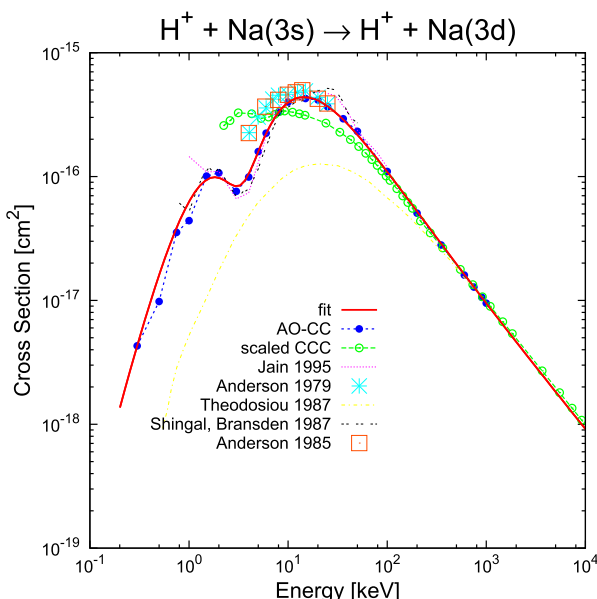
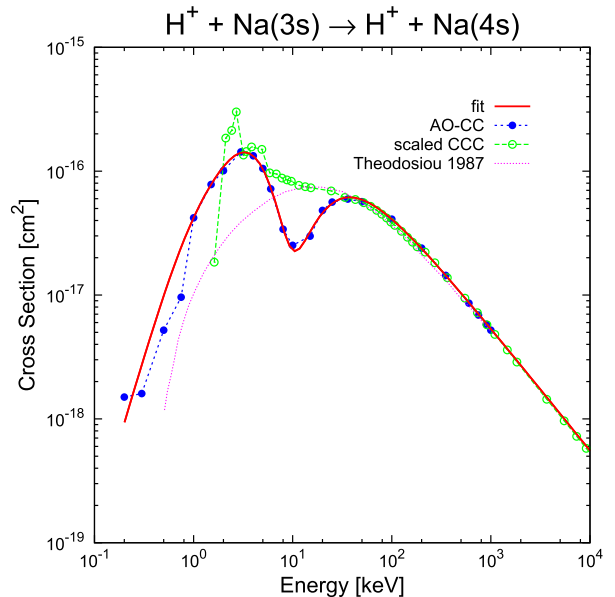
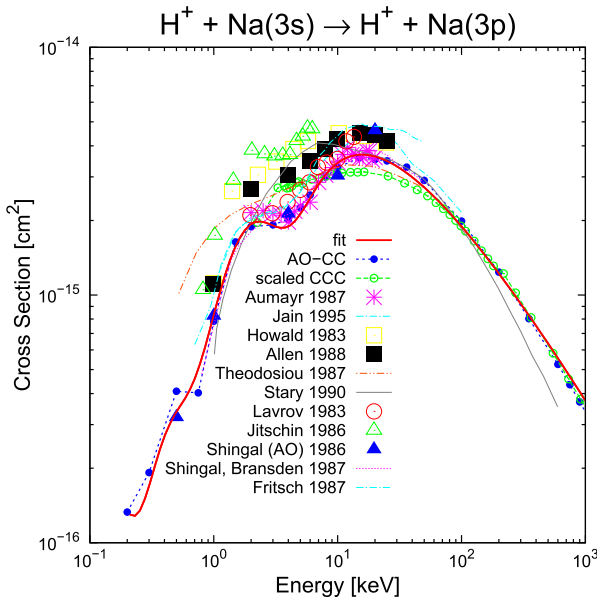
Graph 35.

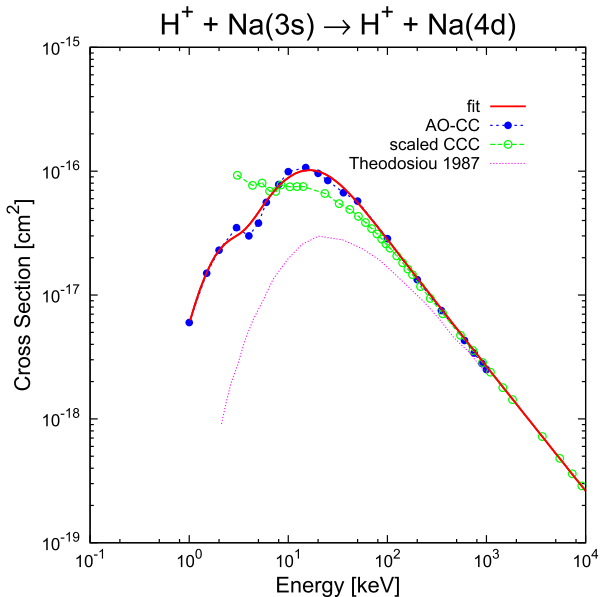


Graph 34.

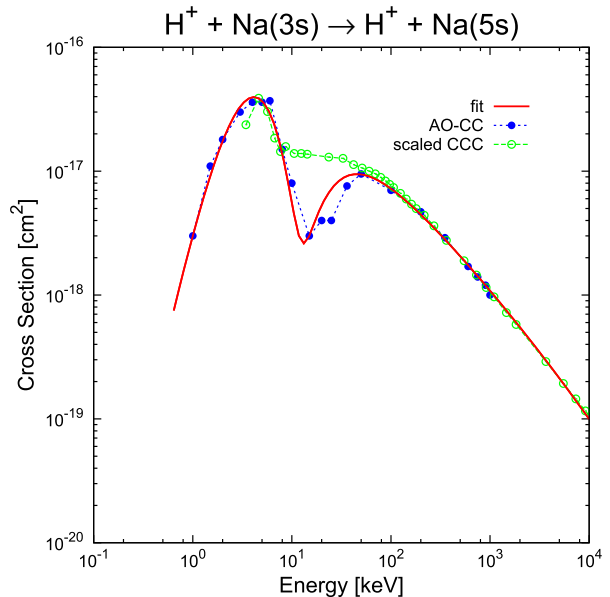


Graph 36.

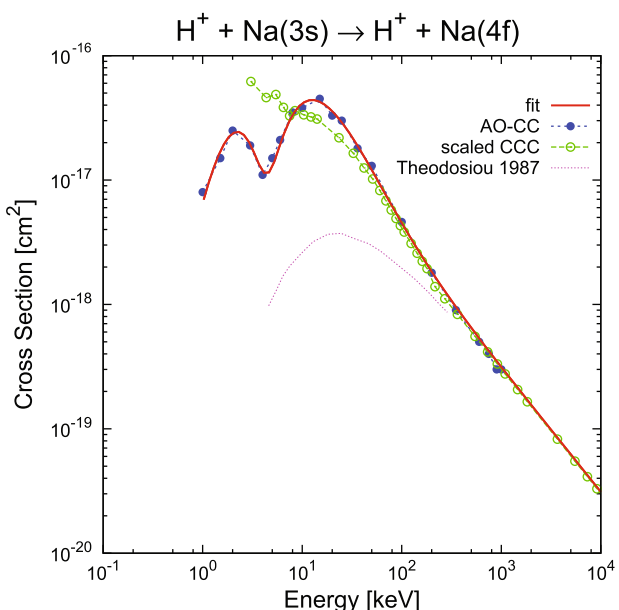




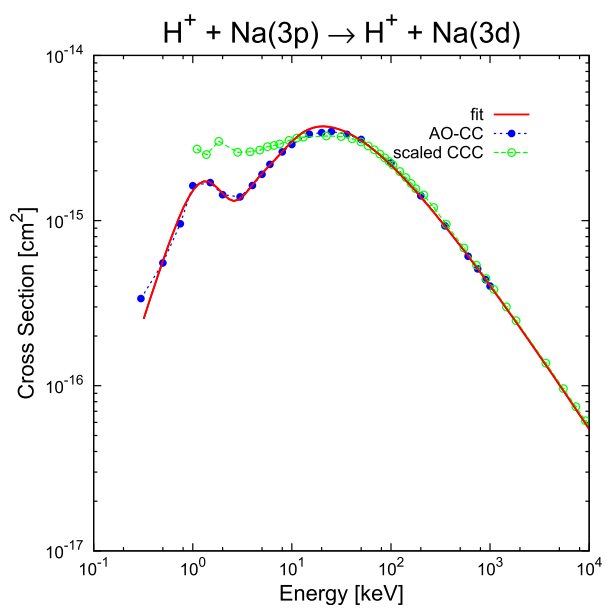
Graph 41.



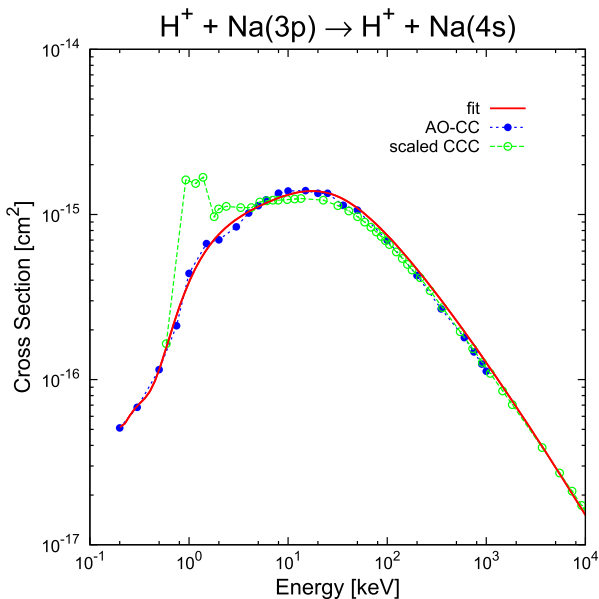
Graph 43.



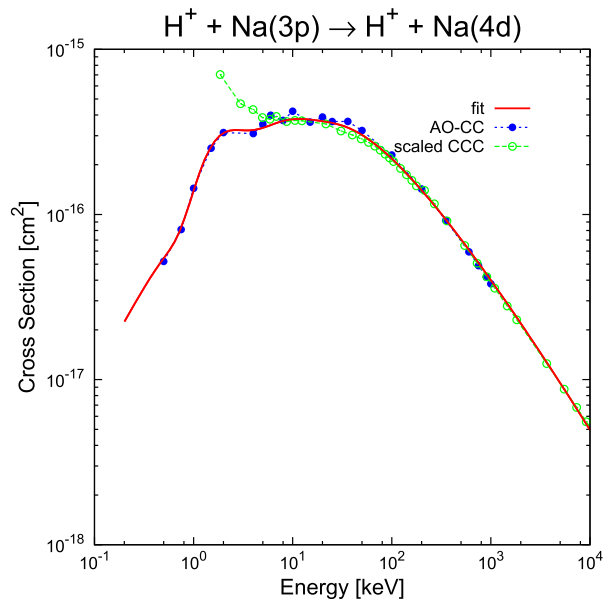
Graph 42.



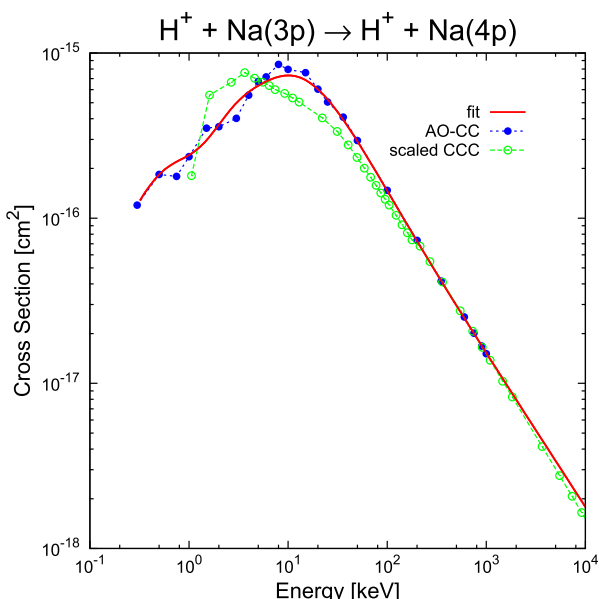
Graph 44.



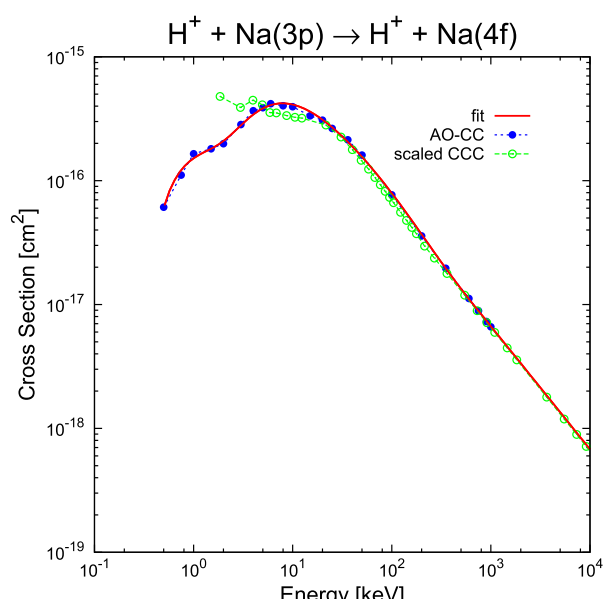
Graph 45.



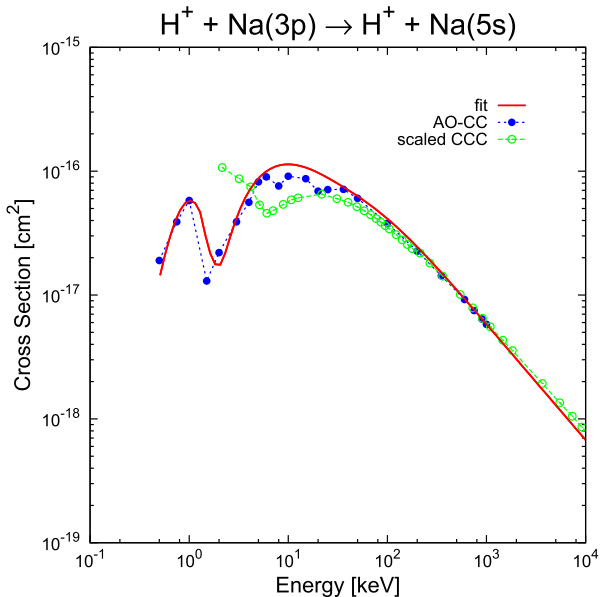
Graph 47.



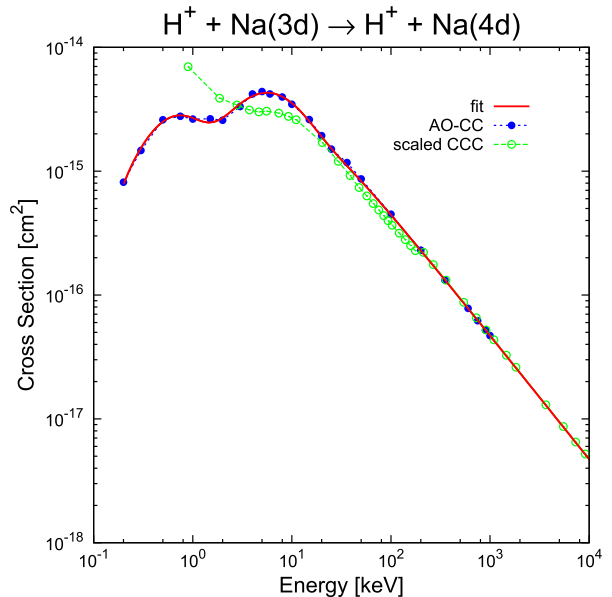
Graph 46.



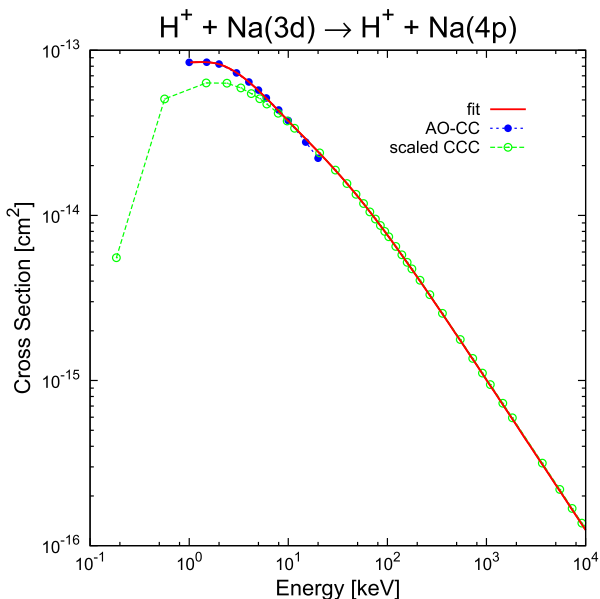
Graph 48.



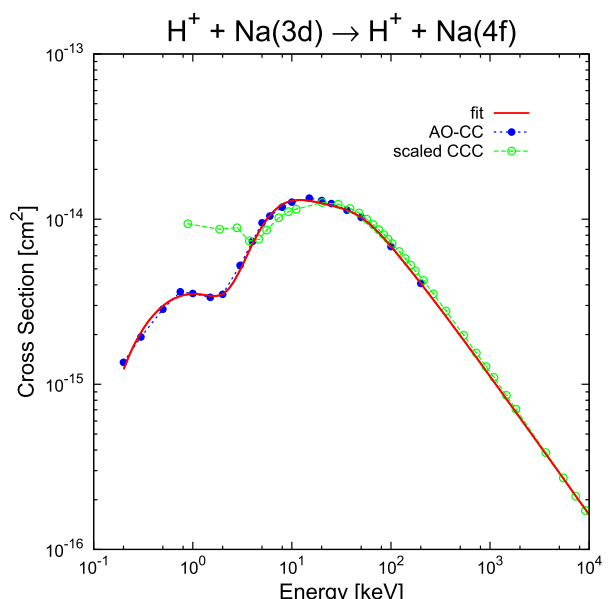
Graph 49.



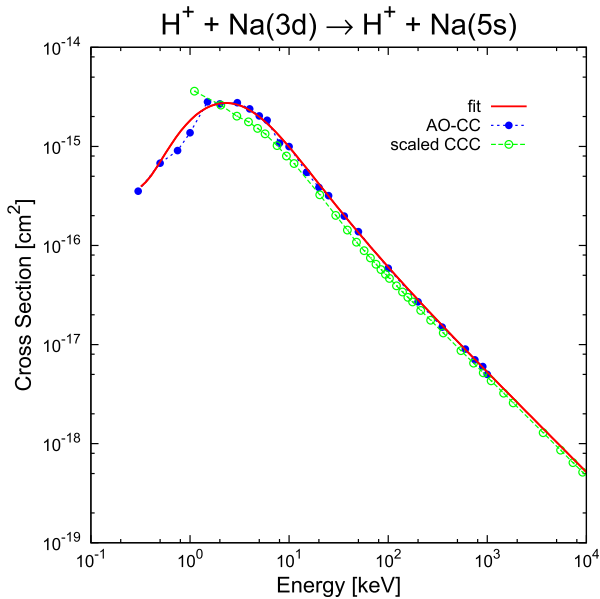
Graph 51.



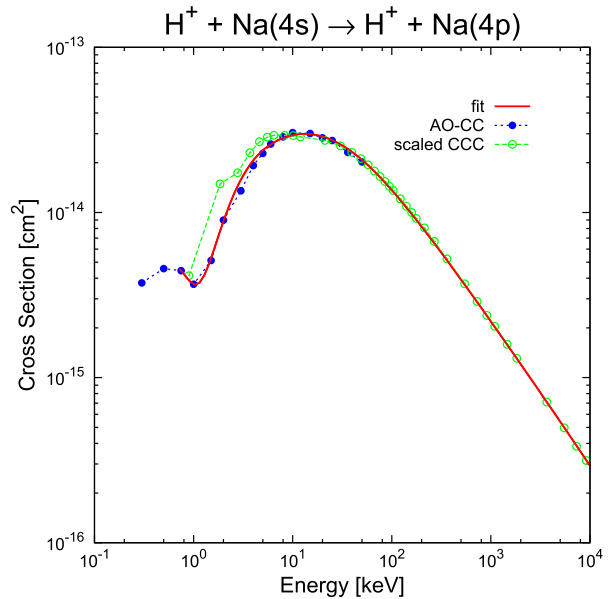
Graph 50.



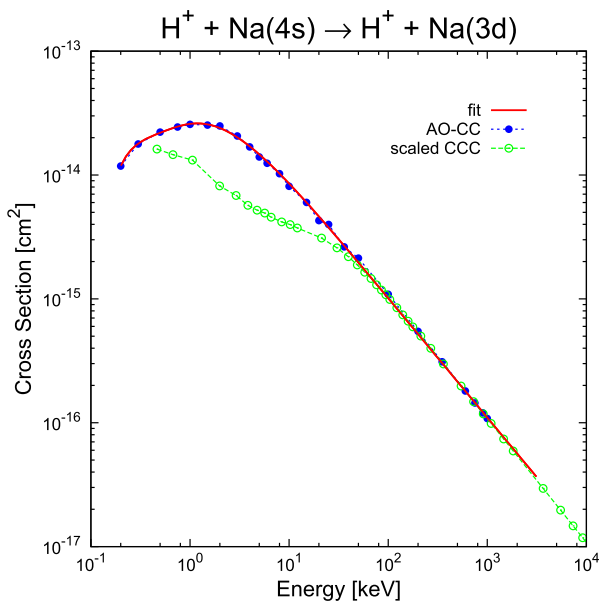
Graph 52.



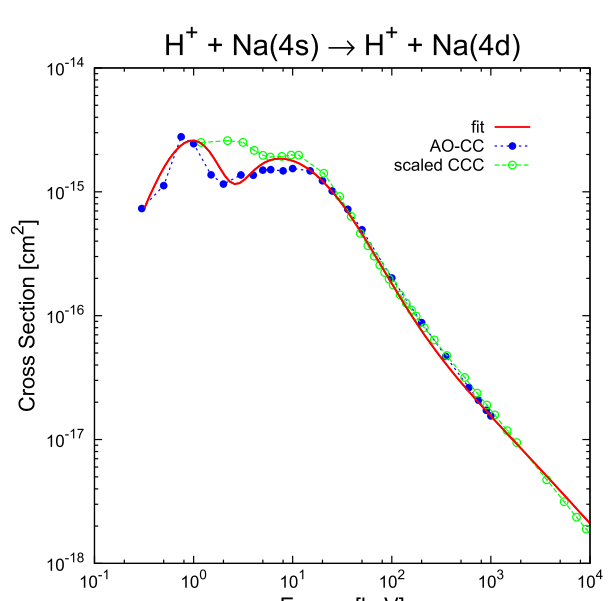
Graph 53.



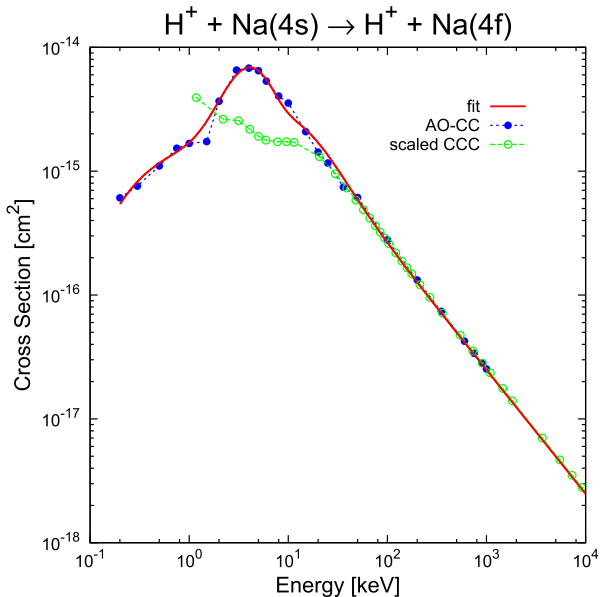
Graph 55.



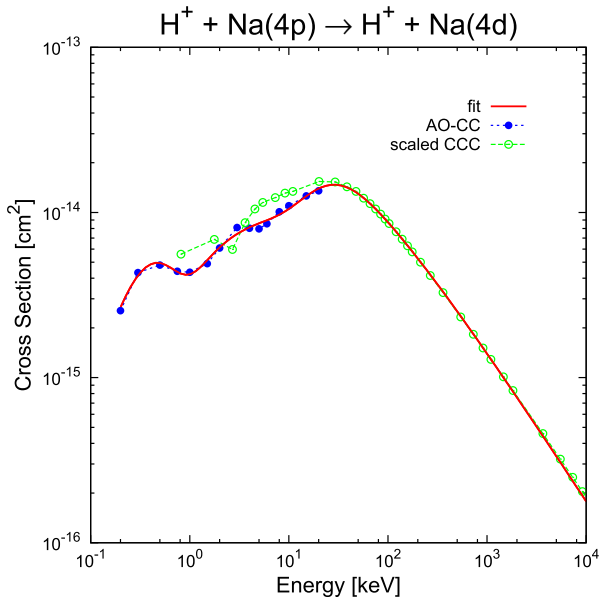
Graph 54.



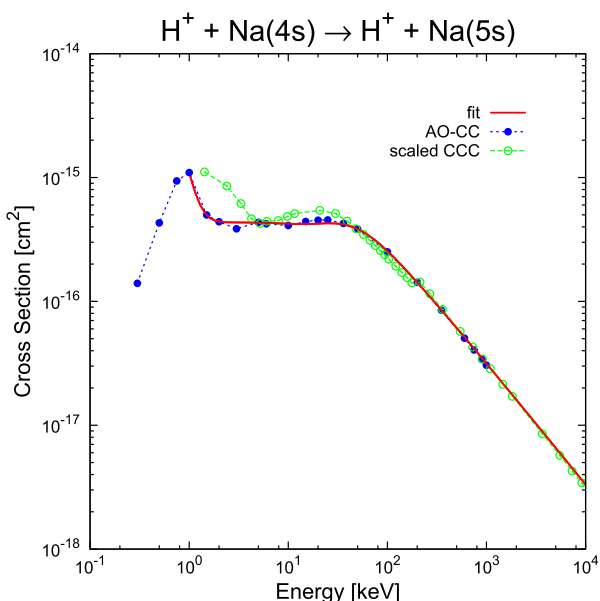
Graph 56.



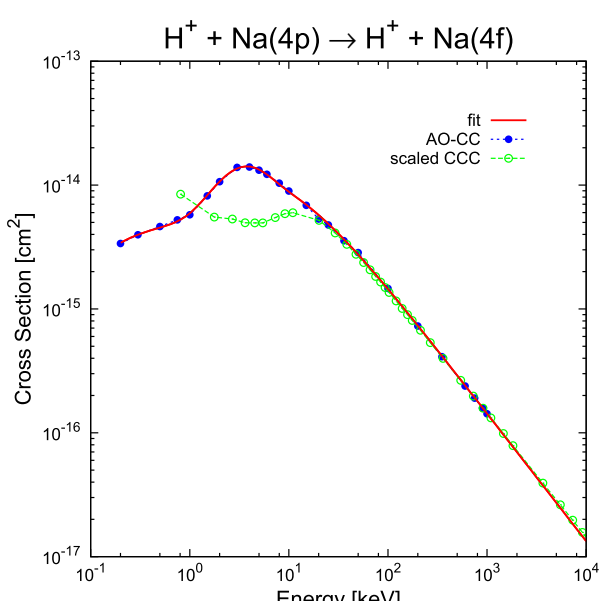
Graph 57.



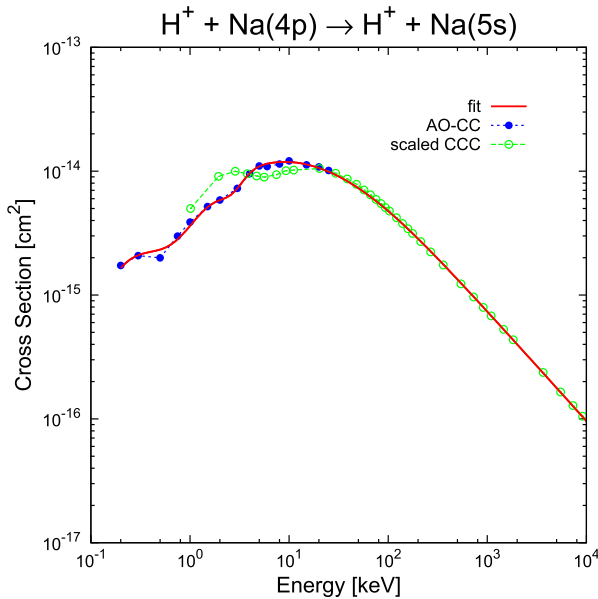
Graph 59.



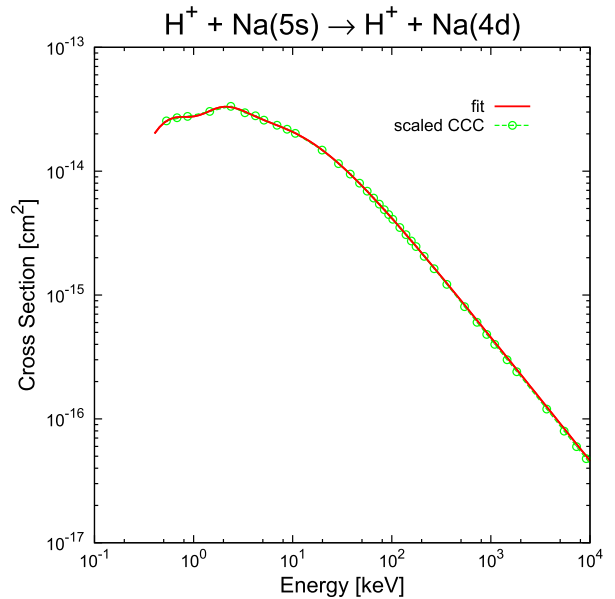
Graph 58.



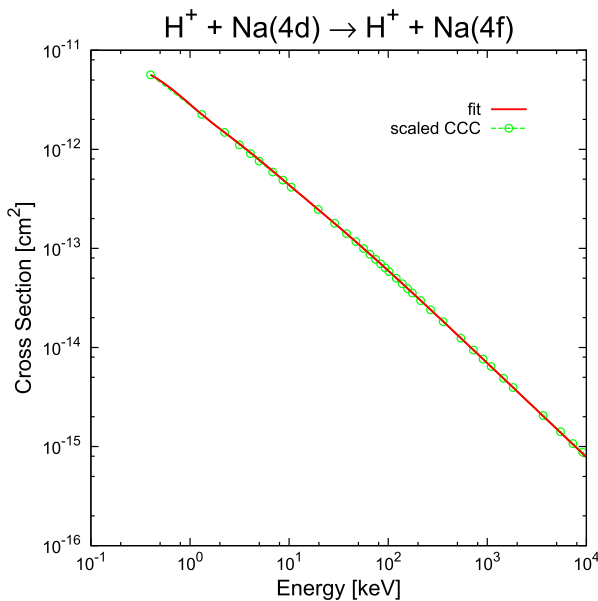
Graph 60.



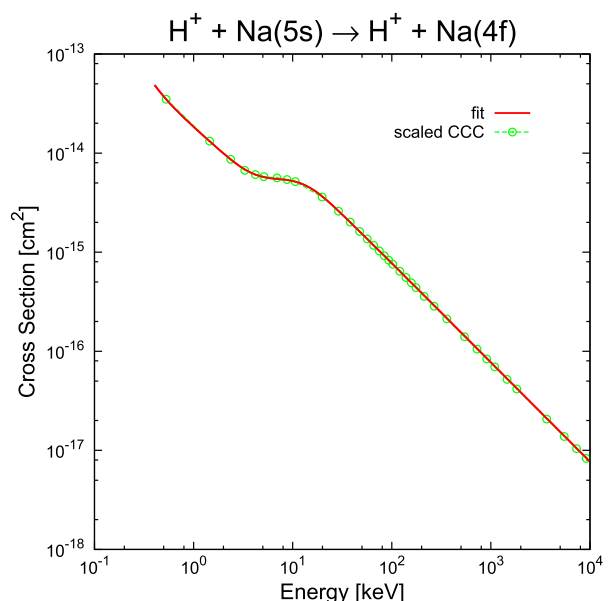
Graph 61.



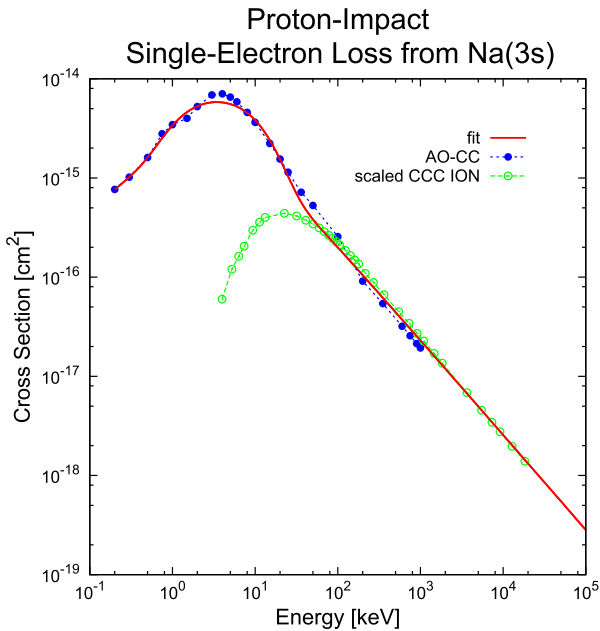
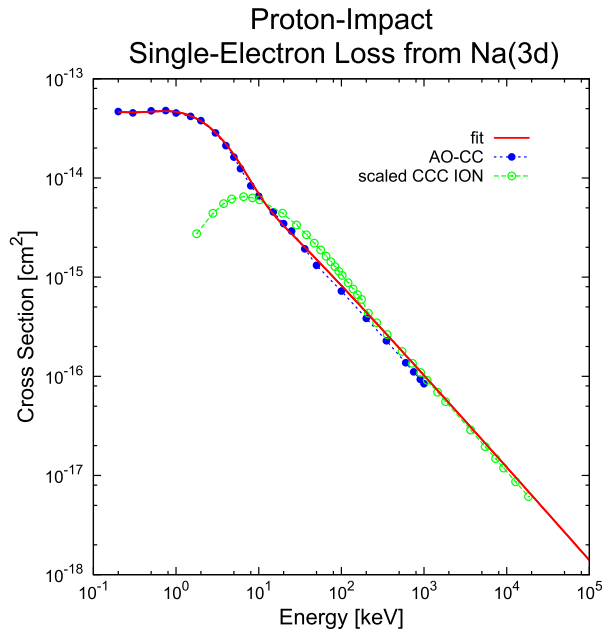
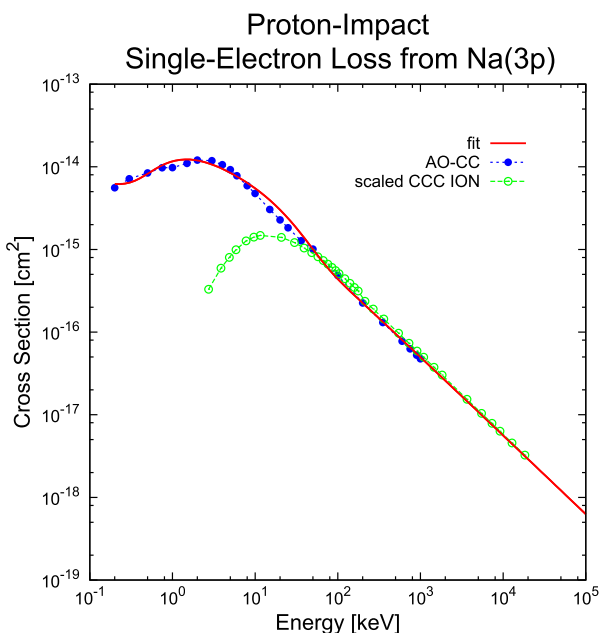
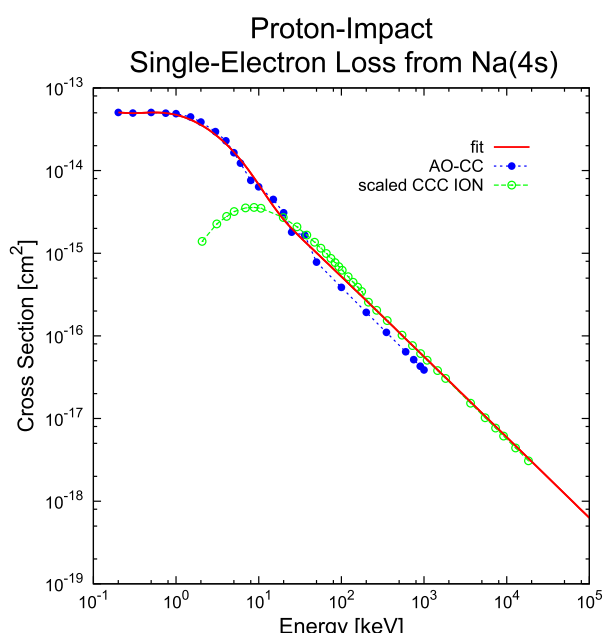
Graph 63.

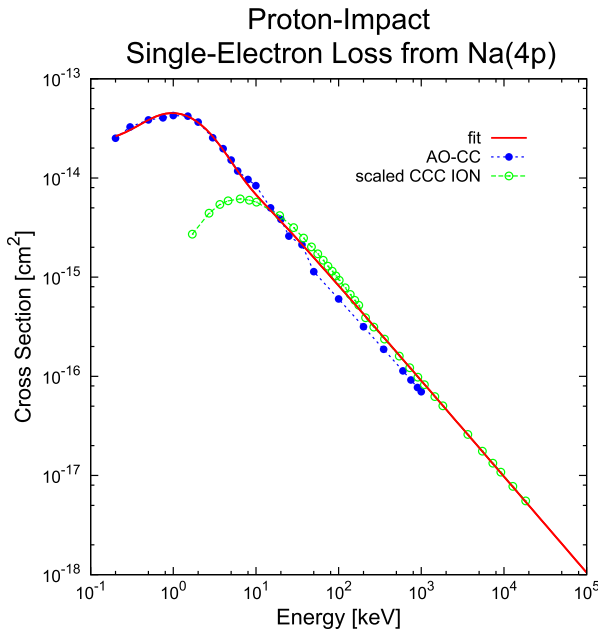
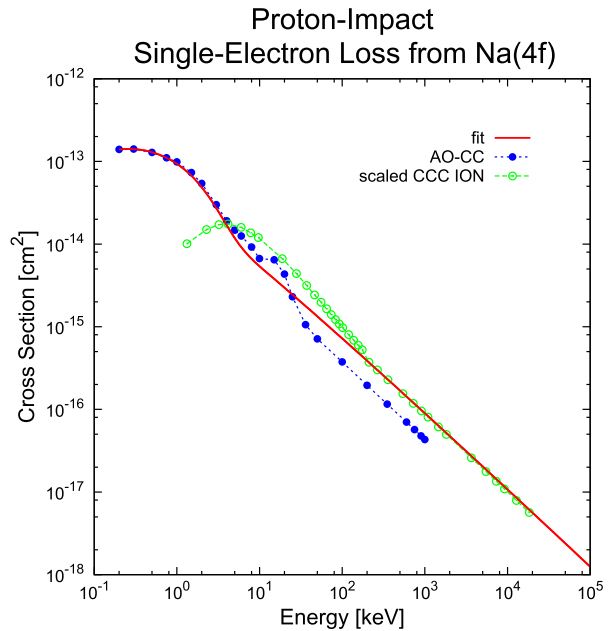
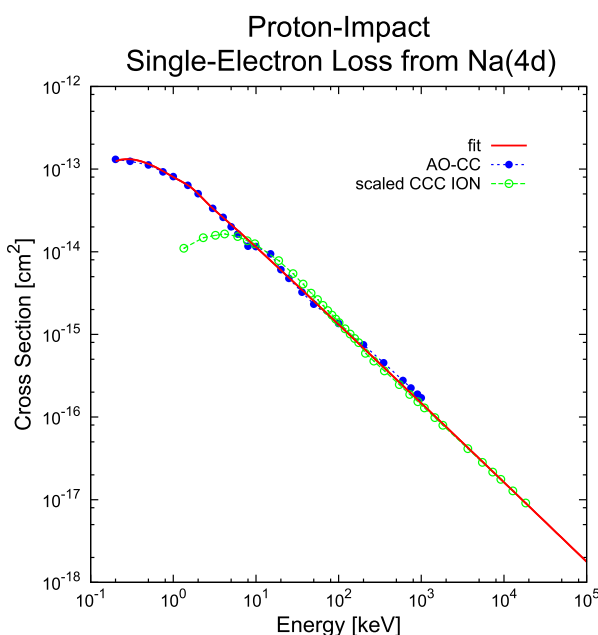
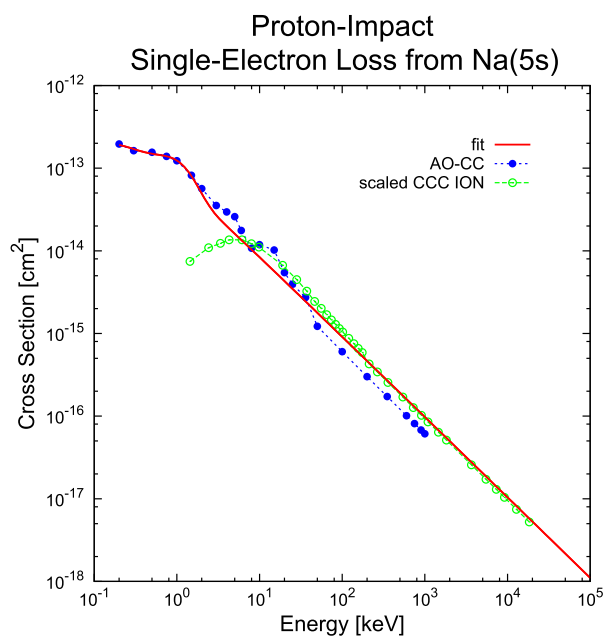


Graph 62.



Graph 64.

**Graph 65.****Graph 67.****Graph 66.****Graph 68.**

**Graph 69.****Graph 71.****Graph 70.****Graph 72.**